

# Type IIB flux vacua from G-theory I

Philip Candelas,<sup>a</sup> Andrei Constantin,<sup>b</sup> Cesar Damian,<sup>c</sup> Magdalena Larfors<sup>b</sup>  
and Jose Francisco Morales<sup>d</sup>

<sup>a</sup>Mathematical Institute, University of Oxford,  
Andrew Wiles Building, Radcliffe Observatory Quarter,  
Woodstock Road, Oxford, OX2 6GG, U.K.

<sup>b</sup>Department of Physics and Astronomy, Uppsala University,  
SE-751 20, Uppsala, Sweden

<sup>c</sup>Departamento de Física, DCI, Campus Leon, Universidad de Guanajuato,  
C.P. 37150, Leon, Guanajuato, Mexico

<sup>d</sup>INFN — Sezione di Roma “TorVergata”, Dipartimento di Fisica,  
Università di Roma “TorVergata”, Via della Ricerca Scientifica, 00133 Roma, Italy  
E-mail: [candelas@maths.ox.ac.uk](mailto:candelas@maths.ox.ac.uk), [andrei.constantin@physics.uu.se](mailto:andrei.constantin@physics.uu.se),  
[cesaredas@fisica.ugto.mx](mailto:cesaredas@fisica.ugto.mx), [magdalena.larfors@physics.uu.se](mailto:magdalena.larfors@physics.uu.se),  
[francisco.morales@roma2.infn.it](mailto:francisco.morales@roma2.infn.it)

**ABSTRACT:** We construct non-perturbatively exact four-dimensional Minkowski vacua of type IIB string theory with non-trivial fluxes. These solutions are found by gluing together, consistently with U-duality, local solutions of type IIB supergravity on  $T^4 \times \mathbb{C}$  with the metric, dilaton and flux potentials varying along  $\mathbb{C}$  and the flux potentials oriented along  $T^4$ . We focus on solutions locally related via U-duality to non-compact Ricci-flat geometries. More general solutions and a complete analysis of the supersymmetry equations are presented in the companion paper [1]. We build a precise dictionary between fluxes in the global solutions and the geometry of an auxiliary  $K3$  surface fibered over  $\mathbb{CP}^1$ . In the spirit of F-theory, the flux potentials are expressed in terms of locally holomorphic functions that parametrize the complex structure moduli space of the  $K3$  fiber in the auxiliary geometry. The brane content is inferred from the monodromy data around the degeneration points of the fiber.

**KEYWORDS:** Flux compactifications, Superstring Vacua, String Duality

ARXIV EPRINT: [1411.4785](https://arxiv.org/abs/1411.4785)

---

**Contents**

<b>1</b>	<b>Introduction</b>	<b>2</b>
<b>2</b>	<b>Local flux solutions dual to Calabi-Yau geometries</b>	<b>4</b>
2.1	The ansatz	4
2.2	Non-compact Calabi-Yau geometries	4
2.3	T and S dualities	6
2.4	Flux solutions	6
<b>3</b>	<b>Global 4d supersymmetric solutions</b>	<b>7</b>
3.1	BPS solutions and moduli spaces	8
3.2	From 6d to 4d	9
3.3	The field/geometry dictionary	10
<b>4</b>	<b>The auxiliary <math>K3</math> surface and its moduli space</b>	<b>11</b>
4.1	The $K3$ fiber	11
4.2	The periods and the $K3$ moduli space	12
4.2.1	The fundamental period	13
4.2.2	The periods	14
4.2.3	$j$ -invariants	15
<b>5</b>	<b>Geometry to flux dictionary</b>	<b>17</b>
5.1	$K3$ -fibered Calabi-Yau threefolds and brane solutions	17
5.1.1	Calabi-Yau threefolds: a first example	17
5.1.2	The brane content	18
5.1.3	Calabi-Yau threefolds: a second example	21
5.2	The $\eta \rightarrow 0$ limit	21
<b>6</b>	<b>Other examples of auxiliary CY threefolds</b>	<b>24</b>
6.1	The second $K3$ surface	25
6.1.1	The moduli space	25
6.1.2	Geometry to flux dictionary	28
6.2	The third $K3$	28
6.2.1	The moduli space	28
6.2.2	Geometry to flux dictionary	30
<b>7</b>	<b>Conclusions and outlook</b>	<b>31</b>
<b>A</b>	<b>A brief review of toric geometry</b>	<b>32</b>
<b>B</b>	<b>The <math>K3</math> moduli space — A more detailed presentation</b>	<b>34</b>
B.1	The discriminant locus	34
B.2	The period computation: Picard-Fuchs equations and the method of Frobenius	35

<b>C Elliptic fibration structures</b>	<b>38</b>
<b>D <math>K3</math> surfaces with Picard number 18 and two complex structures</b>	<b>38</b>

---

## 1 Introduction

In the presence of fluxes, supersymmetry requires that the internal manifold of a type II string compactification be of generalised complex type. Even though the requirements for supersymmetric flux vacua have been known for a long time [2], it is still challenging to find explicit solutions when the four-dimensional spacetime is Minkowski. In a compact space, the charge and tension associated with fluxes must be balanced by the introduction of branes and O-plane sources [3]. The back reaction of these objects on the compact geometry should be consistently included in the picture. These localised defects act as delta-like sources in the equations of motion for the supergravity fields, that, as a consequence, can seldom be solved in an analytic form.<sup>1</sup>

The aim of the present paper is to present explicit examples of non-perturbatively exact supersymmetric four-dimensional Minkowski vacua where all the fields can be written out in an analytic form even in the presence of fluxes. To achieve this, we follow the strategy used in refs. [5, 6], where type IIB supergravity backgrounds describing systems of 3-branes and 7-branes on  $K3$  were described in purely geometric terms.

The strategy is inspired by F-theory [7], where backgrounds with 7-branes are described in terms of elliptic fibrations. The complex structure parameter of the fiber plays the role of the axio-dilaton field  $\tau$  of type IIB theory and the degeneration points of the fiber indicate the presence of brane sources. On the other hand, the  $SL(2, \mathbb{Z})$  self-duality group of type IIB string theory in ten dimensions is identified with the modular group of the elliptic fiber. In compactifications to lower dimensions, the number of scalars is larger and the U-duality group bigger. Remarkably, as shown in [5, 6], the moduli space of six dimensional solutions can be put in correspondence with the moduli space of complex structures of certain  $K3$  surfaces, and the flux solutions can be geometrized in terms of auxiliary  $K3$ -fibered Calabi-Yau threefolds having the  $K3$  in question as a fiber. Similar studies where the U-duality groups of type II theories compactified to lower dimensions have been geometrized can be found in [8–34].

The resulting geometrical picture is analogous to the F-theory picture: the torus has simply been replaced by a  $K3$ . The  $SL(2, \mathbb{Z})$  modular group of the elliptic fiber is replaced by the U-duality group  $SO(2, n, \mathbb{Z})$  acting on the space of complex structures of the  $K3$  fiber. The structure of singularities is richer, allowing for monodromies associated to brane charges of various types and dimensions. The subtle question of tadpole cancelation, which is a major impediment in the construction of type II vacua, is automatically solved

---

<sup>1</sup>The best understood examples involve warped Calabi-Yau geometries with anti-self dual 3-form fluxes [4]. The warp factor is governed by a harmonic equation in the compact space sourced by fluxes, branes and O-planes that can be typically solved only locally in the region of weak string coupling.

by holomorphicity. Indeed, the monodromy around a contour enclosing all singularities is by construction trivial showing that all brane charges add up to zero. In particular, this implies that all solutions include exotic brane objects [35] that at weak coupling should recombine into O-planes. Like in F-theory, all these subtle features of the background are nicely encoded in the auxiliary geometry. The complex plane closes up into a two-sphere for configurations involving a number of 24 branes. The resulting four-dimensional vacua can then be viewed as purely geometric solutions of a gravity theory, dubbed *G-theory* in [6], compactified on a *K3* fibration over  $\mathbb{CP}^1$ .

In the present work, we focus on compactifications of the type IIB string on compact six-dimensional manifolds that are locally isomorphic to  $T^4 \times \mathbb{C}$  and consider fluxes of a more general type. We construct explicit solutions falling into the familiar class of warped Calabi-Yau geometries with anti-self-dual three-form fluxes and two classes of solutions that are warped complex but non-Kähler. The three classes, that we will refer to as A, B, and C, describe systems of 3,7-branes and 5-branes of NSNS and RR types respectively. In this paper, we restrict ourselves to solutions related to Calabi-Yau geometries via U-dualities. These solutions are completely characterised in terms of up to three holomorphic functions. In the companion paper [1], we will present a general analysis of the supersymmetry equations and their solutions, providing examples that are not related to purely metric backgrounds by means of U-dualities.

We stress that the solutions found are, like their F-theory analogs, non-perturbatively exact. Indeed, the expansion of the supergravity fields around any of the branching points always exhibits, beside the logarithmic singularity, an infinite tower of instanton-like corrections. Generically, the solutions correspond to non-geometric U-folds from the ten-dimensional perspective, since the metric of the internal space, and other supergravity fields, are in general patched up by non-geometric U-duality transformations (see [20] for a recent review on non-geometry in string compactifications). Similar ideas were exploited years ago in [10] to describe solutions with non-trivial  $H = dB$  field, but vanishing RR fluxes, in terms of elliptic fibrations.

The paper is organised as follows. In section 2, we derive three classes of local solutions with non-trivial fluxes. We start from a flux-less Ricci flat non-compact background describing a fibration of  $T^4$  over  $\mathbb{C}$  and then, through a sequence of S and T dualities, we obtain flux solutions. In section 3 we discuss the global completion of the local solutions. We exploit the observation that the  $n$  holomorphic functions characterising the local solutions parametrize a double coset space that turns out to be isomorphic to the moduli space of complex structures of algebraic *K3* surfaces<sup>2</sup> with Picard number  $20 - n$ . The flux solutions can then be described in terms of an auxiliary threefold with *K3* fiber and  $\mathbb{CP}^1$  base (the complex plane plus the point at infinity). In section 4 we discuss the complex structure moduli space for a simple choice of *K3* surface with  $n = 2$  complex structure parameters, which serves as our main example. In section 5 we work out the details of the flux/geometry dictionary for various explicit examples of Calabi-Yau threefolds whose fiber

---

<sup>2</sup>An algebraic *K3* is a surface that can be holomorphically embedded in  $\mathbb{CP}^m$ , for some  $m$ , by polynomial equations.

is the algebraic  $K3$  surface studied in section 4. We use the language of toric geometry, in which the fibration structure of a Calabi-Yau three-fold is specified by a reflexive 4d polytope containing a 3d reflexive sub-polytope associated to a  $K3$  with  $n$  complex deformations. The holomorphic functions defining the flux vacua are identified with periods of the holomorphic two-form of the  $K3$  fiber. We compute the periods and extract the brane content from their monodromies around the points where the complex structure of the  $K3$  fiber degenerates. In section 6 we present two other examples of  $K3$  surfaces with Picard number 18 and using these, we construct  $K3$ -fibered Calabi-Yau threefolds and discuss the associated flux solutions. The paper is supplemented by four appendices. In appendix A, we review the main elements of toric geometry needed for our analysis. Appendix B contains the more technical details concerning the analysis of the moduli space for the main example, while appendix C lists the five different elliptic fibration structures for this  $K3$  surface. Finally, in appendix D we list the 8 other  $K3$  surfaces with Picard number 18 and 2 complex structures that are present in the Kreuzer-Skarke list.

## 2 Local flux solutions dual to Calabi-Yau geometries

### 2.1 The ansatz

In this section we construct a class of type IIB solutions on space-times  $\mathbb{R}^{1,3} \times M_6$ , with  $M_6$  a non-compact manifold with topology  $T^4 \times \mathbb{C}$ . These solutions form a sub-class of the more general solutions presented in [1]. The metric of the torus  $g_{mn}$ , the dilaton  $\phi$ , the Neveu-Schwarz (NSNS)  $B$ -field and Ramond-Ramond (RR)  $C_p$ -fields are assumed to vary over  $\mathbb{C}$ . All the non-trivial fluxes are assumed to be oriented along  $T^4$ .

Let  $\{y^1, y^2, y^3, y^4\}$  be real coordinates on  $T^4$  and  $z$  a complex coordinate on  $\mathbb{C}$ . In these coordinates, the metric and the fluxes have the generic form:

$$\begin{aligned}
 ds^2 &= ds_4^2 + ds_6^2 = e^{2A} \sum_{\mu=0}^3 dx_\mu dx^\mu + \sum_{m,n=1}^4 g_{mn} dy^m dy^n + 2e^{2D} |h(z)|^2 dz d\bar{z} \quad (2.1) \\
 B &= \frac{1}{2} b_{mn} dy^m \wedge dy^n, \quad C_2 = \frac{1}{2} c_{mn} dy^m \wedge dy^n, \quad C_4 = c_4 dy^1 \wedge dy^2 \wedge dy^3 \wedge dy^4,
 \end{aligned}$$

with  $A, D, g_{mn}, b_{mn}, c_{mn}, c_4, C_0$  and  $\phi$  varying only over the complex plane.

### 2.2 Non-compact Calabi-Yau geometries

In the absence of fluxes, supersymmetry requires that the internal six-dimensional manifold be of Calabi-Yau type. A six-dimensional Calabi-Yau manifold is characterised by the existence of a closed two-form  $J$  and a closed holomorphic three-form  $\Omega_3$ , that define a Kähler structure and, respectively, a complex structure. A family of closed forms defining Ricci-flat Kähler metrics can be written as

$$\begin{aligned}
 \Omega_3 &= h dz \wedge [(dy^4 - \tau dy^1) \wedge (dy^3 - \sigma dy^2) - \beta (dy^1 \wedge dy^4 - dy^2 \wedge dy^3) - \beta^2 dy^1 \wedge dy^2] \\
 J &= dy^1 \wedge dy^4 + dy^2 \wedge dy^3 + \frac{i}{2} e^{2D} |h|^2 dz \wedge d\bar{z} \quad (2.2)
 \end{aligned}$$

with

$$e^{2D} = \sigma_2 \tau_2 - \beta_2^2, \tag{2.3}$$

and  $\tau = \tau_1 + i \tau_2$ ,  $\sigma = \sigma_1 + i \sigma_2$ ,  $\beta = \beta_1 + i \beta_2$ ,  $h$  arbitrary holomorphic functions of  $z$ . It is easy to see that  $\Omega_3$  and  $J$  given in (2.2) define an  $SU(3)$  structure<sup>3</sup> and are closed,

$$d\Omega_3 = dJ = 0. \tag{2.4}$$

As such, they define a complex structure and a Kähler structure. They also define a metric, which turns out to be Ricci-flat. Explicitly, the metric can be written as [36] (see also [37])

$$g_{MN} = -J_{MP} I^P{}_N. \tag{2.5}$$

where  $I$  is a complex structure induced by  $\Omega_3$ :

$$I^P{}_N = c \epsilon^{PM_1 \dots M_5} (\text{Re } \Omega_3)_{NM_1 M_2} (\text{Re } \Omega_3)_{M_3 M_4 M_5}, \tag{2.6}$$

and the normalisation constant  $c$  is fixed by the requirement  $I_M{}^P I_P{}^N = -\delta_M^N$ .

Substituting (2.2) into (2.5), one finds the metric as

$$ds_6^2 = g_{mn} dy^m dy^n + 2e^{2D} |h|^2 dz d\bar{z} \tag{2.7}$$

with

$$g_{mn} = e^{-2D} \begin{pmatrix} \sigma_2 & \beta_2 & \beta_2 \sigma_1 - \beta_1 \sigma_2 & -\beta_1 \beta_2 + \sigma_2 \tau_1 \\ \beta_2 & \tau_2 & -\beta_1 \beta_2 + \sigma_1 \tau_2 & \beta_2 \tau_1 - \beta_1 \tau_2 \\ \beta_2 \sigma_1 - \beta_1 \sigma_2 & -\beta_1 \beta_2 + \sigma_1 \tau_2 & \text{Im}(\bar{\beta}^2 \sigma) + |\sigma|^2 \tau_2 & |\beta|^2 \beta_2 + \text{Im}(\beta \bar{\sigma} \bar{\tau}) \\ -\beta_1 \beta_2 + \sigma_2 \tau_1 & \beta_2 \tau_1 - \beta_1 \tau_2 & |\beta|^2 \beta_2 + \text{Im}(\beta \bar{\sigma} \bar{\tau}) & \text{Im}(\bar{\beta}^2 \tau) + |\tau|^2 \sigma_2 \end{pmatrix} \tag{2.8}$$

The metric (2.8) can be shown to be Ricci-flat for any choice of the holomorphic functions  $\sigma, \tau, \beta, h$  and therefore it defines a local solution of the equations of motion. The sub-class of solutions corresponding to  $\beta = 0$  will be of interest later on. In this case, the Ricci-flat metric takes the simpler form:

$$ds_6^2 = \frac{1}{\tau_2} |dy^1 + \tau dy^4|^2 + \frac{1}{\sigma_2} |dy^2 + \sigma dy^3|^2 + 2\sigma_2 \tau_2 dz d\bar{z} |h|^2 \tag{2.9}$$

and corresponds to a fibration of  $T^2 \times T^2$  over  $\mathbb{C}$  where the complex structures  $\tau, \sigma$  of the two tori vary holomorphically along the plane.

In section 3 we will construct global solutions by extending the definition of the holomorphic functions to the whole complex plane up to non-trivial U-duality monodromies around a finite number of singular points. Moreover, the function  $h$  will be chosen such that the metric along the 2d plane is regular at infinity leading to a compact  $\mathbb{CP}^1$  geometry. The resulting supersymmetric four-dimensional vacuum corresponds to a geometric compactification on a Calabi-Yau threefold, realised as a  $T^4$  fibration over  $\mathbb{CP}^1$ , if these monodromies do not include T-duality transformations. If they do, the compactification is a non-geometric version of a Calabi-Yau three-fold.

---

<sup>3</sup>They satisfy  $\Omega_3 \wedge J = 0$  and  $\frac{i}{8} \Omega_3 \wedge \bar{\Omega}_3 = \frac{1}{6} J \wedge J \wedge J$ .

### 2.3 T and S dualities

The Ricci-flat metric (2.8) can be mapped to flux backgrounds with the help of T and S dualities. Under T-duality along a direction  $y$ , the metric in the string frame and the NSNS/RR fields transform as [38–40]:

$$\begin{aligned}
 g'_{yy} &= \frac{1}{g_{yy}}, & e^{2\phi'} &= \frac{e^{2\phi}}{g_{yy}}, & g'_{ym} &= \frac{B_{ym}}{g_{yy}}, & B'_{ym} &= \frac{g_{ym}}{g_{yy}} \\
 g'_{mn} &= g_{mn} - \frac{g_{my} g_{ny} - B_{my} B_{ny}}{g_{yy}}, & B'_{mn} &= B_{mn} - \frac{B_{my} g_{ny} - g_{my} B_{ny}}{g_{yy}} \\
 C'_{m\dots n\alpha y} &= C_{m\dots n\alpha} - (n-1) \frac{C_{[m\dots n]y} g_{y|\alpha|}}{g_{yy}} \\
 C'_{m\dots n\alpha\beta} &= C_{m\dots n\alpha\beta} - n C_{[m\dots n\alpha} B_{\beta]y} - n(n-1) \frac{C_{[m\dots n]y} B_{|\alpha|y} g_{|\beta]y}}{g_{yy}}
 \end{aligned} \tag{2.10}$$

On the other hand, for backgrounds with  $C_0 = 0$ , the S-duality transformations are

$$\phi' = -\phi \quad g' = e^{-\phi} g \quad C'_2 = -B \quad B' = C_2 . \tag{2.11}$$

### 2.4 Flux solutions

Starting from the metric (2.8) and acting locally with T and S dualities, one can generate local Type IIB solutions with various types of fluxes. We denote the three main classes of solutions as A, B and C with A for warp, B for  $B$ -flux and C for  $C_2$ -flux. They are defined by the maps

$$\text{CY} \xleftrightarrow{T_{12}} \text{B} \xleftrightarrow{S} \text{C} \xleftrightarrow{T_{14}} \text{A} \tag{2.12}$$

The resulting solutions are characterised by the three holomorphic functions  $\sigma, \tau, \beta$ , this time encoding the information about the fluxes rather than the metric.

**A:** The metric is warped flat

$$g_{mn} = e^{\phi-2A} \delta_{mn} \quad e^{2D} = e^{-2A} = \sqrt{\sigma_2 \tau_2 - \beta_2^2} \quad e^{-\phi} = \tau_2 \tag{2.13}$$

The non-trivial fluxes are

$$\begin{aligned}
 C_0 &= \tau_1 \\
 C_4 &= \left( -\sigma_1 + \frac{2\beta_1\beta_2}{\tau_2} - \frac{\tau_1\beta_2^2}{\tau_2^2} \right) dy^1 \wedge dy^2 \wedge dy^3 \wedge dy^4 \\
 B &= -\frac{\beta_2}{\tau_2} (dy^1 \wedge dy^2 - dy^3 \wedge dy^4) \\
 C_2 &= \left( \beta_1 - \frac{\tau_1\beta_2}{\tau_2} \right) (dy^1 \wedge dy^2 - dy^3 \wedge dy^4)
 \end{aligned} \tag{2.14}$$

This solution describes general systems of D3- and D7-branes and their U-dual.<sup>4</sup>

---

<sup>4</sup>The  $B$  and  $C_2$  fluxes are anti-self-dual forms. As such, they go through two-cycles of zero-volume since  $j \wedge \chi_{\bar{a}} = 0$ , for any anti-self-dual two-form  $\chi_{\bar{a}}$ , where  $j$  is the Kähler form on  $T^4$ . The associated brane sources correspond to a D3-brane coming from D5-branes wrapping a vanishing two-cycle on  $T^4$ .

**B:** The metric and dilaton depend on the imaginary parts of three holomorphic functions  $\tau, \sigma$  and  $\beta$ :

$$g = \begin{pmatrix} \tau_2 & -\beta_2 & 0 & 0 \\ -\beta_2 & \sigma_2 & 0 & 0 \\ 0 & 0 & \sigma_2 & -\beta_2 \\ 0 & 0 & -\beta_2 & \tau_2 \end{pmatrix}; \quad A = 0 \quad \text{and} \quad e^{2D} = e^{2\phi} = \sigma_2 \tau_2 - \beta_2^2 \quad (2.15)$$

The real parts of the holomorphic functions specify the non-trivial  $B$ -field components:

$$B = \tau_1 dy^1 \wedge dy^4 + \sigma_1 dy^2 \wedge dy^3 - \beta_1(dy^2 \wedge dy^4 + dy^1 \wedge dy^3) \quad (2.16)$$

This solution describes general systems of intersecting NS5-branes and their U-duals.

**C:** This solution is found from B exchanging the NS and RR two-forms and preserving the metric in the Einstein frame. One finds

$$g = e^{2A} \begin{pmatrix} \tau_2 & -\beta_2 & 0 & 0 \\ -\beta_2 & \sigma_2 & 0 & 0 \\ 0 & 0 & \sigma_2 & -\beta_2 \\ 0 & 0 & -\beta_2 & \tau_2 \end{pmatrix}, \quad e^{2D} = e^{-2A} = e^{-\phi} = \sqrt{\sigma_2 \tau_2 - \beta_2^2} \quad (2.17)$$

The real parts of the holomorphic functions specify the non-trivial  $C_2$ -field components

$$C_2 = \tau_1 dy^1 \wedge dy^4 + \sigma_1 dy^2 \wedge dy^3 - \beta_1(dy^2 \wedge dy^4 + dy^1 \wedge dy^3) \quad (2.18)$$

This solution describes general systems of intersecting D5-branes and their U-duals.

In [1], we present generalisations of solutions A, B and C preserving the same supersymmetry charges, but involving fluxes of a more general type. In particular, we present examples of solutions of A, B and C characterised by  $n > 3$  holomorphic solutions that cannot be related to a purely metric background via U-duality.

### 3 Global 4d supersymmetric solutions

In the previous section, we solved the supersymmetric vacuum equations of type IIB supergravity without sources. This led us to local solutions characterised by a set of holomorphic functions. In order to define a global four-dimensional solution with Minkowski vacuum, branes and orientifold planes are needed in order to balance the charge and tension contributions of the fluxes in the internal manifold [3]. In our solutions, we will introduce the branes and O-planes as point-like sources in the  $\mathbb{C}$ -plane, over which the four-torus is fibered. The monodromies around these points exhibited by the local holomorphic functions specify the brane content.



### 3.1 BPS solutions and moduli spaces

The solutions under consideration can be viewed as supersymmetric solutions of  $\mathcal{N} = (2, 2)$  maximal supergravity in six dimensions with a number of scalar fields varying over the  $z$ -plane. The scalar manifold of the maximal supergravity in six-dimensions is the homogeneous space

$$\mathcal{M}_{\text{IIB on } T^4} = \text{SO}(5, 5, \mathbb{Z}) \backslash \frac{\text{SO}(5, 5, \mathbb{R})}{\text{SO}(5, \mathbb{R}) \times \text{SO}(5, \mathbb{R})} \quad (3.1)$$

understood as a double coset. This space has dimension 25: 9 coming from the symmetric and traceless metric on  $T^4$ ,  $2 \times 6$  from NSNS and RR two-forms and 4 from the dilaton, the RR zero- and four-forms. The set of holomorphic fields entering in the supersymmetric solutions of classes A, B and C found in the previous section and described in their full generality in [1], span a complex submanifold of (3.1). The precise submanifold can be identified from the U-duality transformation properties of the various fields (see [5] for a detailed discussion).

The solutions found in the previous section involved a number of  $n \leq 3$  locally holomorphic functions parametrizing the  $n$ -complex dimensional submanifold

$$\mathcal{M}_{\text{BPS}} = \text{SO}(2, n, \mathbb{Z}) \backslash \frac{\text{SO}(2, n, \mathbb{R})}{\text{SO}(2, \mathbb{R}) \times \text{SO}(n, \mathbb{R})} \subset \mathcal{M}_{\text{IIB on } T^4} \quad (3.2)$$

The U-duality group  $\text{SO}(2, 3, \mathbb{Z})$  is generated by

$$S : \tau \longrightarrow -\frac{1}{\tau}, \quad \sigma \longrightarrow \sigma - \frac{1}{2\tau} \beta^2, \quad \beta \longrightarrow \frac{1}{\tau} \beta \quad (3.3)$$

$$T : \tau \longrightarrow \tau + 1 \quad (3.4)$$

$$W : \beta \longrightarrow \beta + 1 \quad (3.5)$$

$$R : \sigma \longleftrightarrow \tau \quad (3.6)$$

Indeed, in the frame of solution A,  $S$  and  $T$  generate the type IIB  $\text{SL}(2, \mathbb{Z})$  self-duality,  $W$  is the axionic symmetry and  $R$  is the T-duality along the four directions of the torus exchanging D3 and D7 branes. Solutions in the B and C classes are related to solutions in the A-class by S- and T-dualities and correspond to different orientations of  $\mathcal{M}_{\text{BPS}}$  inside the coset space  $\mathcal{M}_{\text{IIB on } T^4}$ .

The moduli space (3.2) has complex dimension  $n$  and is isomorphic to the moduli space of complex structures on an algebraic  $K3$  surface with Picard number  $20 - n$ , which we denote by  $\mathcal{M}_{K3, n}$  [41]. The holomorphic functions involved in these solutions are defined on the complex plane up to non-trivial actions of the  $\text{SO}(2, n, \mathbb{Z})$  U-duality group.

In the case  $n = 2$ , i.e.  $\beta = 0$ , the variables  $\sigma$  and  $\tau$  parametrize the double coset

$$\mathcal{M}_{K3, 2} = O(\Gamma_{2, 2}) \backslash \frac{\text{SO}(2, 2, \mathbb{R})}{\text{SO}(2, \mathbb{R}) \times O(2, \mathbb{R})} \cong \text{SO}(\Gamma_{2, 2}) \backslash \left( \frac{\text{SL}(2, \mathbb{R})}{\text{U}(1)} \right)^2 \quad (3.7)$$

where  $O(\Gamma_{2,2})$  is the group of isometries of the transcendental lattice<sup>5</sup> of the  $K3$  surface in question, or, in the Type IIB language,  $O(\Gamma_{2,2})$  is the U-duality group:

$$O(\Gamma_{2,2}) = \text{SO}(2, 2, \mathbb{Z}) \cong \mathbb{Z}_2 \times \text{SL}(2, \mathbb{Z})_\tau \times \text{SL}(2, \mathbb{Z})_\sigma \tag{3.8}$$

and  $\mathbb{Z}_2$  acts by permuting the two  $\text{SL}(2, \mathbb{R})$  factors. The space (3.7) can be viewed as a  $\mathbb{Z}_2$ -quotient of the space of complex structures of a product of two tori.

In the case  $n = 3$ , the variables  $\sigma, \tau$  and  $\beta$  parametrize the double coset

$$\mathcal{M}_{K3,3} = O(\Gamma_{2,3}) \backslash \frac{\text{SO}(2, 3, \mathbb{R})}{\text{SO}(2, \mathbb{R}) \times \text{SO}(3, \mathbb{R})} \tag{3.9}$$

with

$$O(\Gamma_{2,3}) = \text{SO}(2, 3, \mathbb{Z}) \cong \text{Sp}(4, \mathbb{Z})/\mathbb{Z}_2 \tag{3.10}$$

the U-duality group. Notice that  $\text{Sp}(4, \mathbb{Z})$  is the modular group of genus two surfaces and therefore the solutions in this class can be viewed as a fibration of a genus two-surface over  $\mathbb{C}$ .

### 3.2 From 6d to 4d

The class of solutions considered so far, corresponds to solutions of the six-dimensional supergravity equations of motion on an patch of the complex plane where functions  $(\sigma, \tau, \dots)$  are holomorphic. These functions span a scalar manifold that is isomorphic to the moduli space  $\mathcal{M}_{K3,n}$  of complex structures of a  $K3$  surface with Picard number  $20 - n$ , and can be regarded as coordinates on such a space.

In order to construct a four-dimensional vacuum, we have to extend these functions to the entire complex plane, including the point at infinity. However, given that on a compact space there are no holomorphic functions except for constants, the solution must be singular at certain points and multi-valued around paths that encircle those points. The global consistency of the solution requires that the monodromies experienced by these functions belong to the U-duality group  $\text{SO}(2, n, \mathbb{Z})$ . Indeed, if this is the case, the set of functions  $(\sigma, \tau, \dots)$  can be regarded as a single-valued map from the complex plane to the coset space  $\mathcal{M}_{K3,n}$  and as such they make sense as solutions of Type IIB. Mathematically, we analytically continue the local holomorphic functions to the complex plane with a number of punctures obtained by removing all the singular points. The map

$$\overline{\mathbb{C}} \setminus \{z_1, \dots, z_m\} \xrightarrow{\sigma, \tau, \dots} \mathcal{M}_{K3,n} \tag{3.11}$$

defines a one-dimensional path in the moduli space of complex structures on a  $K3$  with Picard number  $20 - n$ , or, put differently, a  $K3$  fibration over  $\overline{\mathbb{C}} \setminus \{z_1, \dots, z_m\}$ . The set of points  $\{z_1, \dots, z_m\}$  represents the singular locus and  $\overline{\mathbb{C}} = \mathbb{C} \cup \{\infty\}$ .

In the Type IIB picture, the locally holomorphic functions entering in the solutions of classes  $A, B$  and  $C$  are expressed in terms of the dilaton, the metric and the flux potentials.

---

<sup>5</sup>For a  $K3$  surface  $S$ , the transcendental lattice is defined as the orthogonal complement of the Picard group (also called the Picard lattice)  $\text{Pic}(S) = H^2(S, \mathbb{Z}) \cap H^{1,1}(S, \mathbb{Z})$  in  $H^2(S, \mathbb{Z})$ .

In the case where monodromies involve a shift symmetry of the type  $\varphi \rightarrow \varphi + q$ , singularities are associated to brane locations. Indeed, the Bianchi identity shows that a monodromy of this type has to be supplemented by the presence of a delta-like source for the supergravity field associated to  $\varphi$  in order to compensate for its flux [5]. For example, for solutions in the A-class with  $\beta = 0$ ,  $\tau = C_0 + i e^{-\phi}$  and  $\sigma = C_4 + i \text{Vol}(T^4)$  a monodromy

$$\tau \longrightarrow \tau + q_1 \quad \sigma \longrightarrow \sigma + q_2 \quad \text{with} \quad q_1, q_2 \in \mathbb{Z} \tag{3.12}$$

around the point  $z_0$ , indicates the presence of  $q_1$  D7-branes and  $q_2$  D3-branes at the point  $z_0$ . In general, we will say that a brane of charge  $(q_1, q_2)$  is located at  $z_0$ .

On the other hand, the presence of a brane curves the plane (brane tension) generating a deficit angle of  $\pi/6$  in the metric [42]. When a critical number of 24 branes is reached, the plane curls up into a two sphere. In order to construct four-dimensional solutions, we will restrict to this critical case, and thus require that the two-dimensional metric satisfies

$$\lim_{z \rightarrow \infty} e^{2D} |h(z)|^2 dz d\bar{z} \sim \frac{dz d\bar{z}}{|z|^4}. \tag{3.13}$$

In this case, the topology of the six-dimensional compact space can be viewed as a  $T^4$  fibration over  $S^2$ . The U-duality invariance of the metric requires that  $e^{2D}|h(z)|^2$  be invariant under U-duality monodromies. This completely fixes the function  $h(z)$ . For  $n = 2$ , where  $e^{2D} = \sigma_2 \tau_2$ , an invariant metric with the asymptotic behaviour (3.13) is produced by the choice [5]

$$h(z) = \frac{\eta(\tau)^2 \eta(\sigma)^2}{\prod_{i=1}^{24} (z - z_i)^{\frac{1}{12}}} \tag{3.14}$$

with  $z_i$  the points where either  $\sigma$  or  $\tau$  degenerates, corresponding to elementary brane charges  $(0, 1)$  or  $(1, 0)$ , respectively. Indeed, by going around a path that encircles a brane of charge  $(q_1, q_2)$  at  $z_0$ , the holomorphic function  $h$  returns to its original value, since the phase produced by the factor  $(z - z_0)^{(q_1 + q_2)/12}$  in the denominator of (3.14) cancels against an identical contribution from the transformations of the Dedekind functions in the numerator under (3.12).

In the case  $n = 3$ , where  $e^{2D} = \sigma_2 \tau_2 - \beta_2^2$ , an invariant combination can be written as

$$h(z) = \left( \frac{\chi_{12}(\Pi)}{\prod_{i=1}^{24} (z - z_i)} \right)^{\frac{1}{12}} \tag{3.15}$$

with  $\chi_{12}(\Pi)$  the cusp form of weight 12 of the genus two surface with period matrix  $\Pi = \begin{pmatrix} \sigma & \beta \\ \beta & \tau \end{pmatrix}$ . Notice that for  $\beta$  small  $\chi_{12}(\Pi) \rightarrow \eta(\tau)^{24} \eta(\sigma)^{24}$  and (3.15) reduces to (3.14) corresponding to the degeneration of a genus two Riemann surface into two genus one surfaces. The three-parameter solution can then be seen as a deformation of the two-parameter one.

### 3.3 The field/geometry dictionary

A global flux solution can be constructed by identifying the holomorphic functions present in the local solution with the complex functions describing the complex structure of certain

$K3$  surfaces fibered over a two-sphere. By Torelli's theorem, the moduli space of complex structures on a  $K3$  surface is given by the space of possible periods. Thus we will identify the holomorphic functions specifying the flux solutions with integrals of the holomorphic two-form  $\Omega$  over a basis  $\{e_i\}$  of integral two-cycles spanning the transcendental lattice of the  $K3$ :

$$\varpi_i = \int_{e_i} \Omega . \tag{3.16}$$

In particular, a pair  $(\sigma, \tau)$  or triplet  $(\sigma, \tau, \beta)$  of holomorphic functions parametrizing the double coset spaces (3.2) with  $n = 2, 3$  can be associated to auxiliary geometries corresponding to fibrations of  $K3$  surfaces with Picard numbers 18 and, respectively, 17 over a two-sphere. For convenience, in the examples of the following sections, we will realise such fibration structures using Calabi-Yau threefolds and the language of toric geometry. Our working examples are taken from the class of  $K3$  surfaces realised as hypersurfaces in toric varieties. Following Batyrev's construction [43], the embedding toric variety, as well as the polynomial defining the  $K3$  hypersurface, can be encoded in a pair  $(\nabla, \Delta)$  of dual three-dimensional reflexive polyhedra. The number of complex structures is given by a simple counting of points in the polytopes (see eq. (A.5) in appendix A, where we review the notions of toric geometry needed for the subsequent discussion).

The Kreuzer-Skarke list [44] contains a complete enumeration of all the 4,319 reflexive polyhedra in three-dimensions. Among these, 2 correspond to  $K3$  manifolds with Picard number 19 and  $n = 1$  complex structure parameter, 9 to  $K3$  manifolds with Picard number 18 and  $n = 2$  complex structure parameters, 24 to  $K3$  manifolds with Picard number 17 and  $n = 3$  complex structure parameters and so on. In the following section, we will exploit the well-understood geometry of  $K3$  fibrations in order to build up global supersymmetric solutions with non-trivial fluxes. Then, in section 5, we will discuss the flux/geometry dictionary for some simple choices of auxiliary Calabi-Yau three-fold geometries that can be realised as  $K3$  fibrations over  $\mathbb{C}\mathbb{P}^1$ .

## 4 The auxiliary $K3$ surface and its moduli space

In this section we consider a first example of a  $K3$  surface with two complex structure parameters defined by a pair of dual reflexive polyhedra. We explore its complex structure moduli space by computing the periods of the holomorphic  $(2, 0)$ -form. In the next section, we will embed the  $K3$  polyhedron into different four-dimensional reflexive polytopes encoding different fibrations of the  $K3$  surface over  $\mathbb{C}\mathbb{P}^1$  and discuss the associated geometry to flux dictionary.

### 4.1 The $K3$ fiber

Consider the pair of polyhedra  $(\nabla, \Delta)$  defined by the data collected in table 1. Using the conventions of appendix A,  $\nabla$  specifies the embedding toric variety and  $\Delta$  the Newton polyhedron that defines the homogeneous polynomial whose zero locus defines a  $K3$  surface.

Let  $z_1, \dots, z_6$  denote the homogeneous coordinates of the embedding toric variety, associated to the vertices of  $\nabla$ , as shown in table 1. The two polyhedra  $\nabla$  and  $\Delta$ , shown in

	$\nabla$	$\Delta$	
$z_1$	$w_1 = (1, -1, -1)$	$v_1 = (0, -1, -1)$	$z_1^3 z_2^3$
$z_2$	$w_2 = (-1, -1, -1)$	$v_2 = (0, 0, 1)$	$z_3^3 z_4^3$
$z_3$	$w_3 = (1, -1, 2)$	$v_3 = (0, 1, 0)$	$z_5^3 z_6^3$
$z_4$	$w_4 = (-1, -1, 2)$	$v_4 = (-1, 0, 0)$	$z_2^2 z_4^2 z_6^2$
$z_5$	$w_5 = (1, 2, -1)$	$v_5 = (1, 0, 0)$	$z_1^2 z_3^2 z_5^2$
$z_6$	$w_6 = (-1, 2, -1)$	$v_0 = (0, 0, 0)$	$z_1 z_2 z_3 z_4 z_5 z_6$

**Table 1.** The list of vertices of  $\nabla$  and the list of lattice points in  $\Delta$ . The left hand side labels  $z_1, \dots, z_6$  represent the homogeneous coordinates associated with the vertices of  $\nabla$ . The last column shows the monomials associated with the points of  $\Delta$ .

	$z_1$	$z_2$	$z_3$	$z_4$	$z_5$	$z_6$
$Q_1$	1	1	1	1	1	1
$Q_2$	2	0	1	1	0	2
$Q_3$	0	2	2	0	1	1

**Table 2.** Weight system for the toric variety embedding  $S$ .

figure 1, define a family of  $K3$  hypersurfaces as the zero locus of homogeneous polynomials of the form:

$$\begin{aligned}
 f_{\text{hom}} &= \sum_{a=0}^5 c_a \prod_{i=1}^6 z_i^{\langle w_i^{K3}, v^a \rangle + 1} \\
 &= -c_0 z_1 z_2 z_3 z_4 z_5 z_6 + c_1 z_1^3 z_2^3 + c_2 z_3^3 z_4^3 + c_3 z_5^3 z_6^3 + c_4 z_2^2 z_4^2 z_6^2 + c_5 z_1^2 z_3^2 z_5^2. \quad (4.1)
 \end{aligned}$$

Here  $v_a$  label the points in  $\Delta$  and  $w_i^{K3}$  the vertices of  $\nabla$ . The polynomial is homogeneous with respect to three rescalings, given by the weight system presented in table 2. The weights have been obtained from the three linear relations  $\sum_i Q_a^i w_i^{K3} = 0$  between the vertices of  $\nabla$ .

We notice that  $f_{\text{hom}}$  is invariant under the rescaling  $z_i \rightarrow \lambda_i z_i$  if the coefficients  $c_a$  are also properly rescaled. For instance  $c_1 \rightarrow c_1 / (\lambda_1^3 \lambda_2^3)$ ,  $c_2 \rightarrow c_2 / (\lambda_3^3 \lambda_4^3)$  and so on. We find the following two invariant combinations:

$$\frac{\xi}{27} = \frac{c_1 c_2 c_3}{c_0^3} \quad \text{and} \quad \frac{\eta}{4} = \frac{c_4 c_5}{c_0^2}. \quad (4.2)$$

The numerical factors are included here for later convenience. As discussed in section 4.2.1,  $\xi$  and  $\eta$  can serve as coordinates on the moduli space.

## 4.2 The periods and the $K3$ moduli space

In this section we outline the computation of the periods of the holomorphic  $(2,0)$ -form which play a crucial role in the construction of the global solutions. The more technical details of the computation have been transferred to appendix B.

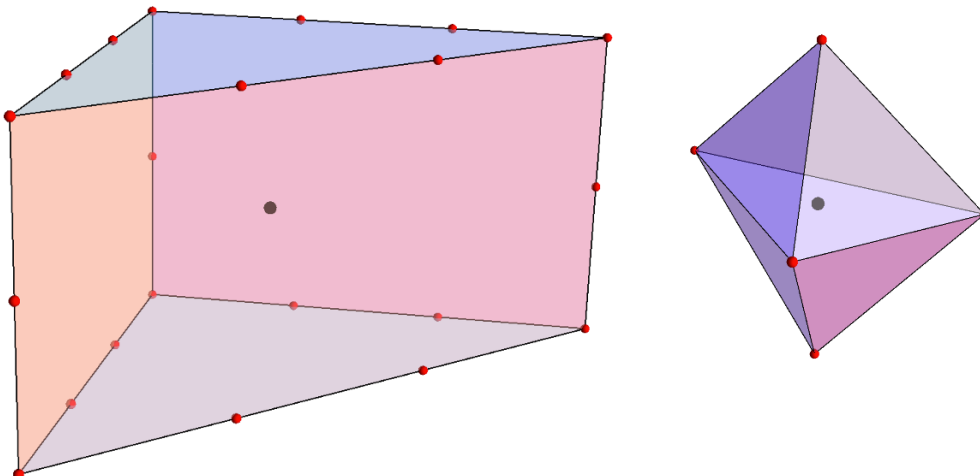


**Figure 1.** The left hand-side polyhedron plays the role of  $\nabla$  and defines the ambient toric variety. For the purpose of clarity, the points that are interior to 2-dimensional faces have been omitted from the plot. The right hand-side polyhedron corresponds to the Newton polyhedron  $\Delta$ .

### 4.2.1 The fundamental period

We are interested in the periods of the holomorphic two-form along the two-cycles spanning the transcendental lattice of the  $K3$  surface. First we compute the fundamental period  $\varpi_{00}$  of the holomorphic two-form by direct integration, as explained in [45] (see also [46–52]). Including a scale factor of  $c_0$ , this is given by:

$$\varpi_{00} = -\frac{c_0}{(2\pi i)^6} \oint_{\mathcal{C}} \frac{dz_1 \wedge \dots \wedge dz_6}{f_{\text{hom}}}, \tag{4.3}$$

where the cycle  $\mathcal{C}$  is a product of small circles that enclose the hypersurfaces  $z_i = 0$ . We rewrite the homogeneous polynomial as

$$f_{\text{hom}} = -c_0 z_1 z_2 z_3 z_4 z_5 z_6 (1 - \tilde{f}_{\text{hom}}). \tag{4.4}$$

The integral (4.3) can be evaluated by residues. We find

$$\varpi_{00}(\xi, \eta) = \frac{1}{(2\pi i)^6} \oint_{\mathcal{C}} \frac{dz_1 \wedge \dots \wedge dz_6}{z_1 z_2 z_3 z_4 z_5 z_6} \sum_{n=0}^{\infty} \tilde{f}_{\text{hom}}^n = \sum_{k,l=0}^{\infty} a_{k,l} \left(\frac{\xi}{27}\right)^k \left(\frac{\eta}{4}\right)^l, \tag{4.5}$$

with

$$a_{k,l} = \frac{\Gamma(3k + 2l + 1)}{\Gamma^3(k + 1) \Gamma^2(l + 1)} \tag{4.6}$$

Only the constant terms in the sum over  $\tilde{f}_{\text{hom}}^n$  contribute to the residue. As expressed in (4.5), these terms are always powers of  $\xi$  and  $\eta$ . The coefficients in the expansion have been obtained from the multinomial theorem.<sup>6</sup>

<sup>6</sup>More explicitly, the expansion involves terms of the form

$$\tilde{f}_{\text{hom}}^n = \left( \frac{\sum_{i=1}^5 c_i z^{p_i}}{c_0 z_1 z_2 z_3 z_4 z_5} \right)^n = \sum_{\substack{n_1 + \dots + n_5 = n \\ n_1 p_1 + \dots + n_5 p_5 = n p_0}} \frac{n!}{\prod_{i=1}^5 n_i!} \cdot \frac{\prod_{i=1}^5 c_i^{n_i}}{c_0^n} + \dots \tag{4.7}$$

### 4.2.2 The periods

Since the number of algebraic 2-cycles is two for this manifold the set of  $\varpi_{00}$  and its derivatives with respect to the parameters  $\xi, \eta$ , contains four linearly independent elements, that is between any six elements of the set  $\{\theta_\xi^i \theta_\eta^j \varpi_{00}\}$ , with  $i + j \leq 2$  where  $\theta_\xi$  and  $\theta_\eta$  denote the operators

$$\theta_\xi = \xi \frac{\partial}{\partial \xi}, \quad \theta_\eta = \eta \frac{\partial}{\partial \eta}, \tag{4.9}$$

there are two linear relations with algebraic, in fact polynomial, coefficients. These linear combinations are the Picard-Fuchs equations. Explicitly, the fundamental period (4.5) satisfies the Picard-Fuchs equations  $\mathcal{L}_1 \varpi_{00} = \mathcal{L}_2 \varpi_{00} = 0$ , with

$$\begin{aligned} \mathcal{L}_1 &= 4\theta_\eta^2 - \eta(3\theta_\xi + 2\theta_\eta + 2)(3\theta_\xi + 2\theta_\eta + 1), \\ \mathcal{L}_2 &= 3\theta_\xi(3\theta_\xi - 2\theta_\eta) - \xi(3\theta_\xi + 2\theta_\eta + 2)(3\theta_\xi + 2\theta_\eta + 1) + 3\eta\theta_\xi(3\theta_\xi + 2\theta_\eta + 1). \end{aligned} \tag{4.10}$$

The equations  $\mathcal{L}_1 \varpi_{00} = \mathcal{L}_2 \varpi_{00} = 0$  can be verified using the series (4.5).

We expect that the differential equations corresponding to  $\mathcal{L}_1$  and  $\mathcal{L}_2$  have four linearly independent common solutions. These can be found using Frobenius' method. Thus we seek four power series that satisfy the differential equations associated to the above Picard-Fuchs operators, of the form

$$\varpi = \sum_{k,l=0}^{\infty} a_{k,l}(\epsilon, \delta) \left(\frac{\xi}{27}\right)^{k+\epsilon} \left(\frac{\eta}{4}\right)^{l+\delta} = \sum_{r,s} \varpi_{r,s} (2\pi i \epsilon)^r (2\pi i \delta)^s. \tag{4.11}$$

As explained in detail in appendix B.2, requiring  $\mathcal{L}_1 \varpi = \mathcal{L}_2 \varpi = 0$ , determines the expansion coefficients to be

$$a_{k,l}(\epsilon, \delta) = \frac{a_{k+\epsilon, l+\delta}}{a_{\epsilon, \delta}} = \frac{\Gamma^3(\epsilon + 1) \Gamma^2(\delta + 1)}{\Gamma(3\epsilon + 2\delta + 1)} \frac{\Gamma(3(k + \epsilon) + 2(l + \delta) + 1)}{\Gamma^3(k + \epsilon + 1) \Gamma^2(l + \delta + 1)}. \tag{4.12}$$

The resulting  $\varpi$  satisfies the Picard-Fuchs equations up to terms proportional to  $\delta^2$  and  $3\epsilon^2 - 2\epsilon\delta$ . We say then that  $\mathcal{L}_1 \varpi = \mathcal{L}_2 \varpi = 0$  hold, if  $\epsilon$  and  $\delta$  satisfy the so-called indicial equations

$$\delta^2 = 0 \qquad 3\epsilon^2 - 2\epsilon\delta = 0. \tag{4.13}$$

It is an important consequence of the indicial relations that all cubic, and higher, monomials in  $\epsilon$  and  $\delta$  vanish. Substituting these relations into (4.11) one finds the finite expansion

$$\varpi = \varpi_{00} + 2\pi i \epsilon \varpi_{10} + 2\pi i \delta \varpi_{01} + (2\pi i)^2 \epsilon \delta \left( \varpi_{11} + \frac{1}{3} \varpi_{20} \right), \tag{4.14}$$

---

where  $p_1 = (3, 3, 0, 0, 0, 0)$ ,  $p_2 = (0, 0, 3, 3, 0, 0)$ ,  $p_3 = (0, 0, 0, 0, 3, 3)$ ,  $p_4 = (2, 2, 2, 0, 0, 0)$ ,  $p_5 = (0, 0, 0, 2, 2, 2)$  and  $p_0 = (1, 1, 1, 1, 1)$ . The omitted terms are non-constant, hence they do not contribute to the residue. Solving the set of equations

$$\begin{aligned} n_1 + \dots + n_5 &= n \\ n_1 p_1 + \dots + n_5 p_5 &= n p_0 \end{aligned} \tag{4.8}$$

we obtain a class of solutions defined by  $n_1 = n_2 = n_3, n_4 = n_5$  and  $n = 3n_1 + 2n_4$ . From these, the invariant combinations (4.2) follow, up to constants.

with each term defining a solution of the Picard-Fuchs equations. Using these, we form the basis

$$\{\varpi_0 = \varpi_{00}, \varpi_1 = \varpi_{10}, \varpi_2 = 3\varpi_{01} + \varpi_{10}, \varpi_3 = 3\varpi_{11} + \varpi_{20}\}, \quad (4.15)$$

which, as explained in appendix B.2, is special in that it leads to the factorisation  $\varpi_0 \varpi_3 = \varpi_1 \varpi_2$ . The quantities  $\varpi_{rs}$  are obtained by taking partial derivatives of the Frobenius period (4.11). Taking partial derivatives produces, on the one hand, logarithms of  $\xi$  and  $\eta$ , and on the other hand, when acting on the  $a_{k,l}$  coefficients, quantities of the form

$$h_{rs} = \frac{1}{(2\pi i)^{r+s}} \sum_{k,l=0}^{\infty} a_{k,l}^{r,s} \left(\frac{\xi}{27}\right)^k \left(\frac{\eta}{4}\right)^l, \quad (4.16)$$

with

$$a_{k,l}^{r,s} = \left(\frac{\partial}{\partial \epsilon}\right)^r \left(\frac{\partial}{\partial \delta}\right)^s a_{k,l}(\epsilon, \delta) \Big|_{\epsilon, \delta=0} \quad (4.17)$$

For the first few terms one finds

$$a_{k,l}^{0,0} = a_{k,l}, \quad a_{k,l}^{0,1} = \frac{a_{k,l}}{2\pi i} (2H_{3k+2l} - 2H_l), \quad a_{k,l}^{1,0} = \frac{a_{k,l}}{2\pi i} (3H_{3k+2l} - 3H_k) \quad (4.18)$$

with  $H_n = \sum_{m=1}^n \frac{1}{m}$  the harmonic numbers. Note that  $h_{00} = \varpi_{00}$ . The basis of periods (4.15) is explicitly given by:

$$\begin{aligned} \varpi_0 &= h_{00} \\ \varpi_1 &= \frac{1}{2\pi i} h_{00} \log\left(\frac{\xi}{27}\right) + h_{10} \\ \varpi_2 &= \frac{1}{2\pi i} h_{00} \log\left(\frac{\xi \eta^3}{1728}\right) + 3h_{01} + h_{10} \\ \varpi_3 &= \frac{1}{(2\pi i)^2} h_{00} \log\left(\frac{\xi}{27}\right) \log\left(\frac{\xi \eta^3}{1728}\right) + \frac{1}{2\pi i} (3h_{01} + h_{10}) \log\left(\frac{\xi}{27}\right) \\ &\quad + \frac{1}{2\pi i} h_{10} \log\left(\frac{\xi \eta^3}{1728}\right) + 3h_{11} + h_{20}. \end{aligned} \quad (4.19)$$

The fact that  $\varpi_0 \varpi_3 = \varpi_1 \varpi_2$  can be checked by multiplication of the respective series. Thus, we can define the complex structure variables  $\tau^{(i)}$  as the period ratios

$$\begin{aligned} \tau^{(1)} &= \frac{\varpi_1}{\varpi_0} = \frac{1}{2\pi i} \log\left(\frac{\xi}{27}\right) + \frac{h_{10}}{h_{00}} \\ \tau^{(2)} &= \frac{\varpi_2}{\varpi_0} = \frac{1}{2\pi i} \log\left(\frac{\xi \eta^3}{1728}\right) + \frac{3h_{01} + h_{10}}{h_{00}}. \end{aligned} \quad (4.20)$$

### 4.2.3 $j$ -invariants

While  $\tau^{(1)}$  and  $\tau^{(2)}$  are defined in terms of  $(\xi, \eta)$  by power series via (4.20), we anticipate that the respective  $j$ -invariants will be algebraically related to  $(\xi, \eta)$ . We start by computing

$$j_1 = j(\tau^{(1)}) \quad j_2 = j(\tau^{(2)}) \quad (4.21)$$



	$\xi = 0$	$\eta = 0$
$\xi j_1$	$\frac{6^3(1-\eta)^3(1-\sqrt{1-\eta})^3}{\eta^3}$	$\frac{3^3(1+8\xi)^3}{(1-\xi)^3}$
$\xi \eta^3 j_2$	$6^3(1-\eta)^3(1+\sqrt{1-\eta})^3$	$12^3(1-\xi)^3$

**Table 3.** The form of  $j_1$  and  $j_2$  along the coordinate lines  $\xi = 0$  and  $\eta = 0$ .

as power series in  $(\xi, \eta)$ , with  $j$  defined as<sup>7</sup>

$$j(\tau) = \frac{E_4^3(\tau)}{\eta^{24}(\tau)} = \epsilon^{-2\pi i \tau} + 744 + \dots \quad q = e^{2\pi i \tau} \quad (4.22)$$

with  $E_n$  the Eisenstein series and  $\eta$  the Dedekind eta function.

Using the small  $\xi, \eta$  expansions one can show that the U-duality invariant combinations  $j_1 j_2$  and  $j_1 + j_2$  are given by rational functions in  $\xi$  and  $\eta$ . Explicitly,

$$\begin{aligned} \frac{1}{6^6} (j_1 - 12^3) (j_2 - 12^3) &= \frac{(8\xi^2 + (\eta - 1)^3 - 12\xi\eta + 20\xi)^2}{\eta^3 \xi^2}, \\ \frac{1}{6^6} j_1 j_2 &= \frac{(8\xi + (\eta - 1)^2)^3}{\eta^3 \xi^2}. \end{aligned} \quad (4.23)$$

Using these relations, one finds the following remarkably simple expressions

$$\begin{aligned} j_1 &= \frac{6^3}{\xi \eta^3} (1 - \xi - \eta - \sqrt{D})^3, \\ j_2 &= \frac{6^3}{\xi \eta^3} (1 - \xi - \eta + \sqrt{D})^3. \end{aligned} \quad (4.24)$$

with  $D$  the discriminant that in our case is given by (see appendix B.1):

$$D = (\xi - 1 - 3\eta)^2 - \eta(\eta + 3)^2. \quad (4.25)$$

The same result can be derived by looking at the loci  $\eta = 0$  and  $\xi = 0$ . The expressions that  $j_1$  and  $j_2$  take along these curves are collected in table 3.

The  $\xi = 0$  column of the table shows that, for general  $(\xi, \eta)$  the quantities  $\xi j_1$  and  $\xi \eta^3 j_2$  cannot be merely rational functions of  $(\xi, \eta)$ . Since, however, all the entries of the table are perfect cubes we can hypothesise that  $(\xi j_1)^{1/3}$  and  $(\xi \eta^3 j_2)^{1/3}$  are of the form

$$\frac{P + Q\sqrt{D}}{R} \quad (4.26)$$

for suitable polynomials  $P, Q$  and  $R$ , where  $D = 0$  corresponds to the discriminant locus, i.e. the locus in moduli space where the K3 is singular. By comparing this form with the series expansions we find again the result (4.24).

<sup>7</sup>Here  $E_{2k}(\tau) = 1 + \frac{2}{\zeta(1-2k)} \sum_{n=1}^{\infty} \frac{n^{2k-1} e^{2n\pi i \tau}}{(1-e^{2n\pi i \tau})}$  with  $\frac{2}{\zeta(-3)} = 240$  and  $\frac{2}{\zeta(-5)} = -504$ . Note also that  $j - 12^3 = \frac{E_6^2}{\eta^{24}}$ .

The above discussion provided us with a number of coordinates on the moduli space (3.2). We started with the parameters  $\xi$  and  $\eta$ , then we found the period ratios  $\tau^{(i)}$  and, finally, we computed the  $SL(2, \mathbb{Z})$ -invariants  $j(\tau^{(i)})$ . We will identify the supergravity fields  $\sigma$  and  $\tau$  entering in the flux solutions with the period ratios  $\tau^{(1)}$  and  $\tau^{(2)}$ , respectively.<sup>8</sup>

In the following section, we will consider one-parameter families of  $K3$  surfaces obtained by treating the coefficients in (4.1), or alternatively, the parameters  $\xi$  and  $\eta$ , as functions of a single complex parameter  $z$ . We will obtain such families by explicitly constructing Calabi-Yau threefolds that are  $K3$  fibrations over  $\mathbb{CP}^1$  using the language of toric geometry.

## 5 Geometry to flux dictionary

### 5.1 $K3$ -fibered Calabi-Yau threefolds and brane solutions

There are many ways in which one can fiber the  $K3$  surface (4.1) over  $\mathbb{CP}^1$  in order to obtain a Calabi-Yau three-fold. Changing the  $K3$  fibration leads to a different brane content in the supergravity solutions. Here we consider two different choices of Calabi-Yau threefolds that have the same  $K3$  fiber and describe the brane content in each case.

#### 5.1.1 Calabi-Yau threefolds: a first example

A three-fold with  $K3$  fiber given by (4.1) can be constructed by starting from the polyhedron  $\nabla_{K3}$  defined by the data presented in table 1, and then extending this polyhedron into a fourth dimension by adding points above and below the hyperplane that contains  $\nabla_{K3}$ . In adding the extra points, one should take care that the resulting four-dimensional polytope  $\nabla_{CY_3}$  is reflexive, and, moreover, that  $\nabla_{K3}$  is contained in  $\nabla_{CY_3}$  as a slice, in the sense explained in section A. The latter condition ensures that the resulting Calabi-Yau three-fold admits a  $K3$  fibration structure with a fiber given by  $\nabla_{K3}$  and its dual.

The simplest extension of  $\nabla_{K3}$  is to add two points, one above and one below the origin, along the extra direction:

$$w_i^{CY_3} = (0, w_i^{K3}) \quad w_7^{CY_3} = (-1, 0, 0, 0) \quad w_8^{CY_3} = (1, 0, 0, 0) \quad (5.1)$$

The resulting Calabi-Yau threefold has Hodge numbers  $(h^{1,1}, h^{2,1}) = (35, 11)$ , as given by Batyrev's formulae [43]. The 8 vertices of  $\nabla_{CY_3}$  define 8 vectors, among which 4 linear relations hold. These lead to the weight system presented in table 4.

The dual polyhedron  $\Delta_{CY_3}$  contains 18 points and leads, via (A.4), to the homogeneous polynomial

$$\begin{aligned} f_{CY_3, \text{hom}} = & (c_{0,1} z_7^2 + c_{0,2} z_7 z_8 + c_{0,3} z_8^2) z_1 z_2 z_3 z_4 z_5 z_6 \\ & + (c_{1,1} z_7^2 + c_{1,2} z_7 z_8 + c_{1,3} z_8^2) z_1^3 z_2^3 + (c_{2,1} z_7^2 + c_{2,2} z_7 z_8 + c_{2,3} z_8^2) z_3^3 z_4^3 \\ & + (c_{3,1} z_7^2 + c_{3,2} z_7 z_8 + c_{3,3} z_8^2) z_5^3 z_6^3 + (c_{4,1} z_7^2 + c_{4,2} z_7 z_8 + c_{4,3} z_8^2) z_2^2 z_4^2 z_6^2 \\ & + (c_{5,1} z_7^2 + c_{5,2} z_7 z_8 + c_{5,3} z_8^2) z_1^2 z_3^2 z_5^2. \end{aligned} \quad (5.2)$$

---

<sup>8</sup>A different order in which  $\sigma$  and  $\tau$  are identified with  $\tau^{(1)}$  and  $\tau^{(2)}$  corresponds to a different solution.

	$z_1$	$z_2$	$z_3$	$z_4$	$z_5$	$z_6$	$z_7$	$z_8$
$Q_1$	1	1	1	1	1	1	0	0
$Q_2$	2	0	1	1	0	2	0	0
$Q_3$	0	2	2	0	1	1	0	0
$Q_4$	0	0	0	0	0	0	1	1

**Table 4.** Weight system for the toric variety embedding the Calabi-Yau three-fold.

The form of the polynomial  $f_{\text{CY}_3, \text{hom}}$  makes manifest the fibration structure. Indeed, we can write it in the form (4.1) but now with the coefficients  $c_a$  replaced by homogenous polynomials of order two in  $z = (z_7, z_8)$  parametrizing the  $\mathbb{CP}^1$  base:

$$f_{\text{CY}_3, \text{hom}} = -c_0(z) z_1 z_2 z_3 z_4 z_5 z_6 + c_1(z) z_1^3 z_2^3 + c_2(z) z_3^3 z_4^3 + c_3(z) z_5^3 z_6^3 + c_4(z) z_2^2 z_4^2 z_6^2 + c_5(z) z_1^2 z_3^2 z_5^2 \tag{5.3}$$

As a result, we can write the parameters  $\xi$  and  $\eta$  defined by (4.2) as functions depending on  $z$ :

$$\frac{\xi(z)}{27} = \frac{f_6(z)}{f_2^3(z)} \quad \text{and} \quad \frac{\eta(z)}{4} = \frac{f_4(z)}{f_2^2(z)}, \tag{5.4}$$

where the subscripts of the polynomials  $f_2(z), f_4(z)$  and  $f_6(z)$  indicate their degree in  $z$ . Explicitly, these polynomials are given by

$$f_2(z) = c_0(z), \quad f_4(z) = c_4(z) c_5(z), \quad f_6(z) = c_1(z) c_2(z) c_3(z). \tag{5.5}$$

### 5.1.2 The brane content

A flux solution of class A, B or C is obtained by identifying the holomorphic functions  $\sigma(z)$  and  $\tau(z)$  characterising the corresponding supergravity solutions with the period ratios  $\tau^{(1)}$  and  $\tau^{(2)}$ . Here we take

$$\sigma(z) = \tau^{(1)}(z) \quad , \quad \tau(z) = \tau^{(2)}(z). \tag{5.6}$$

The  $K3$  fibration discussed in the previous section defines an embedding of the base space  $\mathbb{CP}^1$  into the moduli space  $\mathcal{M}_{K3,2}$  (or equivalently the supergravity scalar manifold) through the map  $z \mapsto (\sigma(z), \tau(z))$ , defined by the composition of (4.20) and (5.4).

The map  $z \mapsto (\xi(z), \eta(z))$  is easier to visualise and, as such, it can give us a more immediate picture of the embedding of the  $\mathbb{CP}^1$  base of the Calabi-Yau threefold into the complex structure moduli space of the  $K3$  fiber. For the chosen Calabi-Yau threefold, figure 2 illustrates this embedding in a schematic way.

In this section, we will infer the brane content of the flux solution from the geometry of the  $K3$  fibration. Branes are located at the poles of  $j_1, j_2$ . A simple inspection of (4.24) shows that these poles are located at the zeros of  $\xi(z)$  and  $\eta(z)$ . To find the orders of these poles, we can expand  $j_1$  and  $j_2$  for small  $\xi$  and, separately, for small  $\eta$ . The exact forms that the  $j$ -functions take in these limits are given in table 3. From this we see that

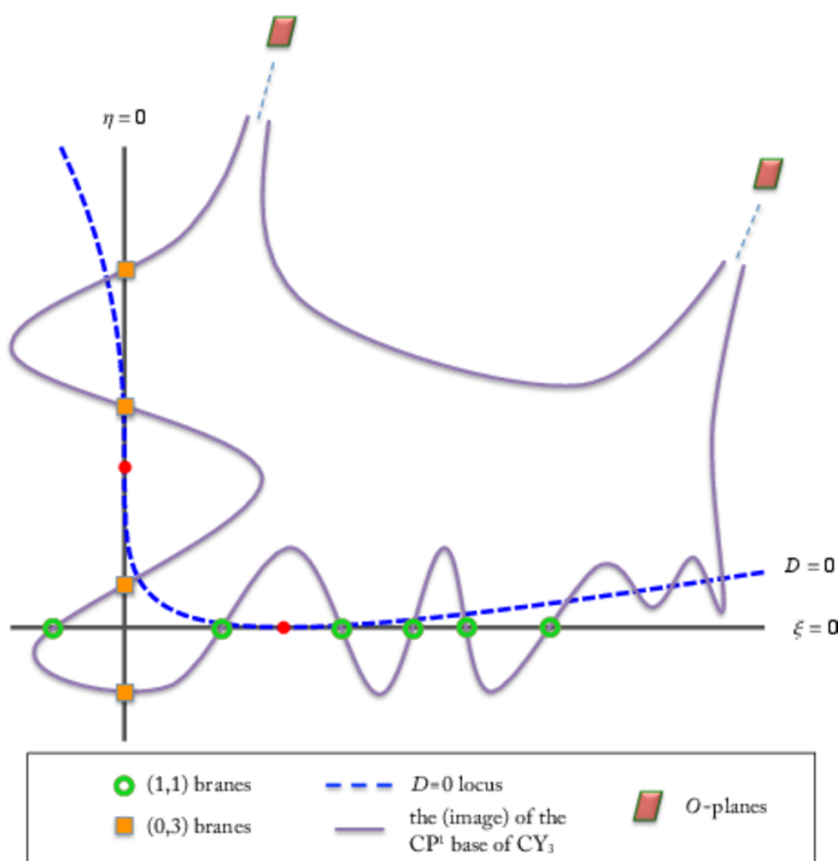


**Figure 2.** The embedding of the (real part of the)  $\mathbb{CP}^1$  base (in purple) of the Calabi-Yau threefold into the complex structure moduli space of the  $K3$  fiber. The green circles and the orange squares correspond to brane locations. The base intersects the  $\xi = 0$  curve in 6 points, the  $\eta = 0$  curve in 4 points and the  $D = 0$  curve in 12 points. At infinity in the  $(\xi, \eta)$ -plane we expect to find O-planes — located at the zeros of  $f_2(z)$  — which cancel the tadpoles associated with the branes.

both  $j_1$  and  $j_2$  have a pole of order 1 along the locus  $\xi = 0$ , while  $j_2$  has a pole of order 3 along  $\eta = 0$ .

The same information can be extracted from the monodromies of  $\tau$  and  $\sigma$ . From (4.20), one finds

$$\sigma, \tau \sim \frac{1}{2\pi i} \log \left( \frac{\xi}{27} \right) . \tag{5.7}$$

at the points where  $\xi(z) = 0$ , which according to eq.(5.4), correspond to the roots of  $f_6$ . Accordingly, if  $\xi(z) \sim (z - z_0)$  has a zero of vanishing order 1 at  $z_0$ , then encircling  $z_0$  one finds the monodromy

$$\sigma \longrightarrow \sigma + 1 \quad \tau \longrightarrow \tau + 1 \tag{5.8}$$

indicating the presence of a brane of charge  $(1, 1)$ , in the sense used in section 3.2. For example, for solutions in the A-class, this corresponds to a bound state of a D7-brane and a D3-brane, while for solutions in classes B and C, to the intersection of 5-branes of NS and R type, respectively. Similarly, if  $f_6$  has a zero with vanishing order  $q$  at  $z_0$ , i.e.

	$f_6$	$f_4$
$(q_1, q_2)$	$(1, 1)$	$(0, 3)$

**Table 5.** Branes of charge  $(q_1, q_2)$  are located at the zeros of  $f_6$  and  $f_4$ .

$f_6(z) = (z - z_0)^q$ , one finds that  $\sigma$  and  $\tau$  exhibit the monodromies associated to a brane of charge  $(q, q)$ . In a count that includes multiplicities, there are 6 points that correspond to branes with charge  $(1, 1)$  in the  $z$ -plane.

Similarly, around the points where  $\eta = 0$ , corresponding to the roots of  $f_4$ , we have

$$\sigma \longrightarrow \sigma + 3 \tag{5.9}$$

indicating the presence of a brane with charge  $(0, 3)$ . We have a total of 4 such points.

The results are summarised in table 5 and illustrated in figure 2. In total, we have  $6 \times 2 + 4 \times 3 = 24$  branes, corresponding the required number for a compact geometry.

Finally, there are 12 points where  $D(\xi(z), \eta(z)) = 0$ , see eq. (4.25). Around these points, there is a  $\mathbb{Z}_2$ -monodromy that interchanges  $j_1$  and  $j_2$ , or, equivalently,  $\tau$  and  $\sigma$  are flipped. The corresponding flux vacuum can therefore be thought of as a non-geometric  $\mathbb{Z}_2$ -orbifold by the U-duality element that flips the two fields.<sup>9</sup>

We can now write down the two-dimensional (holomorphic) metric  $h(z)$ . Following eq. (3.14) and the ensuing remarks, we obtain

$$h(z) = \frac{\eta(\tau)^2 \eta(\sigma)^2}{\prod_{i=1}^6 (z - a_i)^{\frac{1}{6}} \prod_{i=1}^4 (z - b_i)^{\frac{1}{4}}} \tag{5.10}$$

where  $\eta(\tau)$  and  $\eta(\sigma)$  are Dedekind eta functions,  $\{a_i\}$  represent the six roots of  $f_6$  and  $\{b_i\}$  the roots of  $f_4$ . The multiplicity of each point is given by the total charge of the corresponding brane — that is 2 for the roots of  $f_6$  and 3 for the roots of  $f_4$  (see the discussion at the end of section 3.2). This gives a total of 24 points. It is interesting to note that these points correspond to the degeneration of the product of the two  $j$ -functions

$$j_1 j_2 \sim \frac{(8\xi + (\eta - 1)^2)^3}{\xi^2 \eta^3} . \tag{5.11}$$

Notice that this product is U-duality invariant unlike the individual  $j_i$ 's. The function  $h(z)$  is single valued around any of the singular points (brane locations). Moreover, at large  $z$ ,  $h(z) \sim z^{-2}$ , so after changing coordinates to  $1/z$ , the metric becomes  $dz d\bar{z}$ , and it is regular. Consequently, the two dimensions parametrized by  $z$  are compact [42].

Additionally, the combination

$$\tau_2 \sigma_2 |h(z)|^2 \tag{5.12}$$

describing the two-dimensional part of the metric (2.9), is invariant under the U-duality group  $SO(2, 2, \mathbb{Z}) \cong \mathbb{Z}_2 \times SL(2, \mathbb{Z})_\tau \times SL(2, \mathbb{Z})_\sigma$ .

<sup>9</sup>A non-geometric  $\mathbb{Z}_2$ -orbifold involving a quotient by T-duality was constructed in [53].

Finally, let us point out that taking

$$f_4(z) = f_2(z)^2 \quad \text{and} \quad f_6(z) = f_2(z)^3 \quad (5.13)$$

leads to constant  $\sigma, \tau$  over the whole complex plane. This suggests that the zeros of  $f_2(z)$  can be interpreted as the positions of the O-planes that achieve a local tadpole cancellation when branes are exactly located on top of them.

### 5.1.3 Calabi-Yau threefolds: a second example

A different three-fold with the same fiber is obtained by extending the polyhedron  $\nabla_{K3}$  defined in table 1 by adding one point “above” and “below” each of the six vertices of  $\nabla_{K3}$ :

$$w_i^{\text{CY}_3} = (0, w_i^{K3}) \quad w_{6+i}^{\text{CY}_3} = (-1, w_i^{K3}) \quad w_{12+i}^{\text{CY}_3} = (1, w_i^{K3}) \quad i = 1, \dots, 6 \quad (5.14)$$

This extension leads to a Calabi-Yau three-fold with Hodge numbers  $(h^{1,1}, h^{2,1}) = (75, 3)$ .

The dual polyhedron  $\Delta_{\text{CY}_3}$  has 8 points and leads to the following polynomial:

$$\begin{aligned} f_{\text{CY}_3, \text{hom}} = & (c_{0,0} z_7 z_8 z_9 z_{10} z_{11} z_{12} z_{13} z_{14} z_{15} z_{16} z_{17} z_{18} \\ & + c_{0,1} z_7^2 z_9^2 z_{11}^2 z_{13}^2 z_{15}^2 z_{17}^2 + c_{0,2} z_8^2 z_{10}^2 z_{12}^2 z_{14}^2 z_{16}^2 z_{18}^2) z_1 z_2 z_3 z_4 z_5 z_6 \\ & + c_1 z_1^3 z_2^3 z_7^3 z_8^3 z_9^3 z_{10}^3 + c_2 z_3^3 z_4^3 z_{11}^3 z_{12}^3 z_{13}^3 z_{14}^3 + c_3 z_5^3 z_6^3 z_{15}^3 z_{16}^3 z_{17}^3 z_{18}^3 \\ & + c_4 z_1^2 z_3^2 z_5^2 z_7^2 z_8^2 z_{11}^2 z_{12}^2 z_{15}^2 z_{16}^2 + c_5 z_2^2 z_4^2 z_6^2 z_9^2 z_{10}^2 z_{13}^2 z_{14}^2 z_{17}^2 z_{18}^2 . \end{aligned} \quad (5.15)$$

We can write the polynomial (5.15) in the form of the polynomial defining the  $K3$  fiber (4.1), but now with the coefficients  $c_a$  replaced by homogenous polynomials of order two in  $z = (z_7, \dots, z_{18})$  parametrizing the  $\mathbb{CP}^1$  base of the Calabi-Yau threefold. Working in the patch  $z_9 = \dots = z_{18} = 1$ , and setting  $z = (z_7, z_8)$  we can write again  $\xi(z)$  and  $\eta(z)$  in the form (5.4) with  $f_2(z)$  a generic homogeneous polynomial of order 2 and

$$f_4(z) \sim z_7^2 z_8^2 \quad f_6(z) \sim z_7^3 z_8^3 . \quad (5.16)$$

Thus for this choice of auxiliary Calabi-Yau three-fold, the branes found in the previous example collide into two groups each of charge:  $(3, 9) = 3 \times (1, 1) + 2 \times (0, 3)$  located  $z_7 = 0$  and  $z_8 = 0$ .

## 5.2 The $\eta \rightarrow 0$ limit

In order to gain a better understanding of the flux-geometry dictionary, it is instructive to consider the choice  $\eta(z) = 0$ , that is the situation in which the  $\mathbb{CP}^1$  base is embedded along the  $\eta = 0$  curve. Looking at the Calabi-Yau threefolds discussed in the previous section, this limit corresponds to setting  $f_4(z) = c_4(z) c_5(z)$  to 0.

Along this curve,  $j_2 \rightarrow \infty$ , i.e.  $\tau^{(2)} \rightarrow i\infty$ . If we make the identification  $\sigma = \tau^{(1)}$  and  $\tau = \tau^{(2)}$  for solutions in the A-class, where  $\tau = C_0 + i e^{-\phi}$ , this limit corresponds to the weak coupling limit with  $\sigma = C_4 + i \text{Vol}(T^4)$  varying over the plane. Alternatively, the same geometry can be used to describe the large volume limit of a varying axio-dilaton dual solution obtained from the identification  $\tau = \tau^{(1)}$  and  $\sigma = \tau^{(2)}$ .

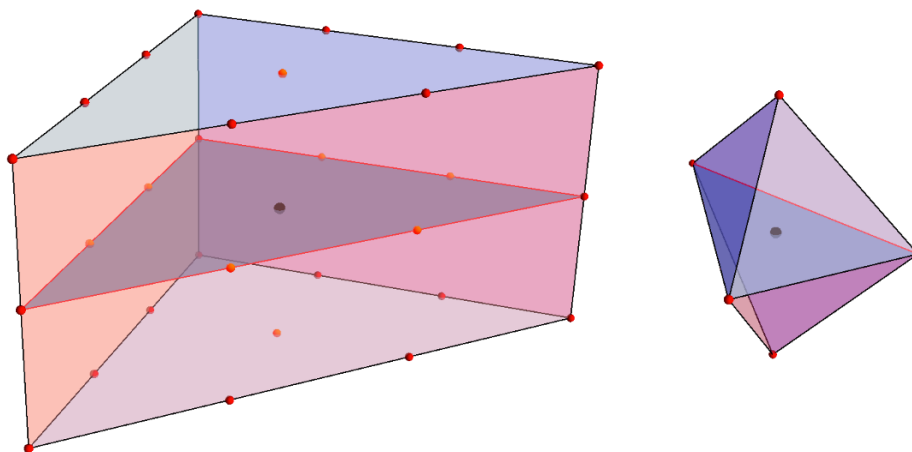


**Figure 3.** The left hand-side polyhedron corresponds to  $\nabla$  and defines the ambient toric variety. All the points are included this time. The polygon passing through the origin corresponds to an elliptic curve and shows that the  $K3$  surface admits an elliptic fibration structure. The points of  $\nabla$  lying on edges and above the polygon form the extended Dynkin diagram of  $SU(9)$ . Similarly, the points below the polygon form and  $SU(9)$  diagram. As such, this fibration structure is of type  $SU(9) \times SU(9)$ . Other elliptic fibration structures for this  $K3$  are listed in appendix C. The right hand-side polyhedron corresponds to the Newton polyhedron  $\Delta$ .

We first notice that in the  $\eta \rightarrow 0$  limits, the sums over  $k$  defining  $\varpi_{00}$  and  $\varpi_{10}$  can be explicitly performed leading to

$$\varpi_{00} = {}_2F_1\left(\frac{1}{3}, \frac{2}{3}, 1, \xi\right) \quad \varpi_{10} = \frac{i}{\sqrt{3}} {}_2F_1\left(\frac{1}{3}, \frac{2}{3}; 1; 1 - \xi\right) \quad (5.17)$$

Thus we have

$$\tau^{(1)} = \frac{\varpi_{10}}{\varpi_{00}} = \frac{i}{\sqrt{3}} \frac{{}_2F_1\left(\frac{1}{3}, \frac{2}{3}; 1; 1 - \xi\right)}{{}_2F_1\left(\frac{1}{3}, \frac{2}{3}; 1; \xi\right)} \quad (5.18)$$

and

$$j_1 = j(\tau_1) = \frac{3^3(1 + 8\xi)^3}{\xi(1 - \xi)^3} . \quad (5.19)$$

Remarkably, eq. (5.18) provides an explicit expression for  $\tau^{(1)}$ . On the other hand, in the limit  $\eta = 0$ ,  $j_1$  develops new poles of order 3 at  $\xi = 1$ . For the Calabi-Yau three folds discussed in the previous section,  $\xi(z)$  has degree 6. As such, we expect to have 18 branes located, in groups of 3, at the zeros of  $\xi(z) - 1$ , and 6 other branes located at the zeros of  $\xi(z)$ .

Moreover one can identify  $j_1$  with the  $j$ -invariant for an elliptic curve ‘contained’ inside the  $K3$  fiber. To this end, consider the pair of polyhedra  $(\nabla, \Delta)$  shown in figure 3 and associate the homogeneous coordinates  $z_1, \dots, z_6$  to the vertices of  $\nabla$  as in section 4.1. In addition, associate three further coordinates with the vertices of the polygon that divides  $\nabla$  into two halves:

$$z_a : (0, -1, -1) \quad z_b : (0, -1, 2) \quad z_c : (0, 2, -1) \quad (5.20)$$

As shown in figure 3, the  $K3$  surface in question admits an elliptic fibration structure. In fact, it admits 5 different fibration structures, as discussed in appendix C. With the above definitions, the defining polynomial, which now makes manifest this elliptic-fibration structure, becomes:

$$\begin{aligned} f_{\text{hom}} &= c_1 z_1^3 z_2^3 z_a^3 + c_2 z_3^3 z_4^3 z_b^3 + c_3 z_5^3 z_6^3 z_c^3 \\ &\quad + (-c_0 z_1 z_2 z_3 z_4 z_5 z_6 + c_4 z_2^2 z_4^2 z_6^2 + c_5 z_1^2 z_3^2 z_5^2) z_a z_b z_c \\ &= a(w) z_a^3 + b(w) z_b^3 + c(w) z_c^3 + d(w) z_a z_b z_c \end{aligned} \tag{5.21}$$

where  $w = (z_1, \dots, z_6)$ . The polynomial (5.21) defines the  $K3$  surface studied in the previous sections as an elliptic fibration over  $\mathbb{CP}^1$ . Now we would like to consider the  $\eta = 0$  direction in the moduli space of this  $K3$  surface, which corresponds to setting  $c_4 = c_5 = 0$ . Along this curve, we have

$$\frac{\xi}{27} = -\frac{a(w) b(w) c(w)}{d(w)^3} = \frac{c_1 c_2 c_3}{c_0^3} . \tag{5.22}$$

Note that the  $w$  dependence drops out from the above expression and, for fixed  $c_0, c_1, c_2, c_3$ , the parameter  $\xi$  is constant along the  $\mathbb{CP}^1$  base of the elliptic fibration. With these identifications, we can proceed to finding the  $j$ -invariant of the elliptic curve defined by

$$a z_a^3 + b z_b^3 + c z_c^3 + d z_a z_b z_c = 0 . \tag{5.23}$$

The polynomial (5.23) can be put in the Weierstrass form<sup>10</sup>  $z_a^2 z_c = z_b^3 + z_b f z_c^2 + g z_c^3$  with

$$f = -\frac{d^4}{48} (8\xi + 1) \quad g = \frac{d^6}{32 \cdot 3^3} (-8\xi^2 - 20\xi + 1) . \tag{5.24}$$

Then the discriminant locus is given by

$$\Delta = 4 f^3 + 27 g^2 = \frac{4 d^{12}}{1728} \xi (1 - \xi)^3 \tag{5.25}$$

and, hence

$$j = 1728 \cdot \frac{4 f^3}{\Delta} = \frac{3^3 (1 + 8\xi)^3}{\xi (1 - \xi)^3} \tag{5.26}$$

exactly matching the expression (5.19). Working, e.g. in the patch  $z_2 = \dots = z_6 = 0$ , we see that  $\Delta$  has degree 24 in  $z_1$  and  $z_2$ , hence we expect 24 points at which  $j$  degenerates.

Further, we can fiber the above  $K3$  surface over  $\mathbb{CP}^1$  as done in sections 5.1.1 and 5.1.3, obtaining polynomials of the form

$$f_{\text{CY}_3, \text{hom}} = a(w, z) z_a^3 + b(w, z) z_b^3 + c(w, z) z_c^3 + d(w, z) z_a z_b z_c \tag{5.27}$$

where  $z$  parametrizes the  $\mathbb{CP}^1$  base over which the  $K3$  surface is fibered. This gives an elliptically fibered Calabi-Yau threefold. However, if we drop the  $w$  dependence, we obtain

---

<sup>10</sup>The expressions for  $f$  and  $g$  were found using Sage (<http://www.sagemath.org>), based on the methods in [54].



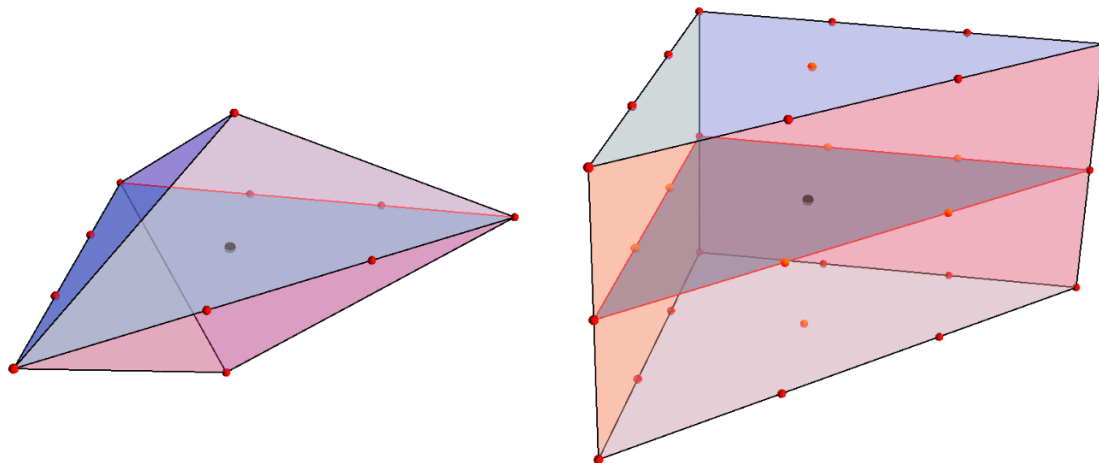


**Figure 4.** The polyhedrons  $\nabla$  associated the  $K3$  surfaces  $\tilde{S}$  for the two choices of Calabi-Yau three-fold embeddings in sections 5.1.1 (left) and 5.1.3 (right).

a second  $K3$  surface, call it  $\tilde{S}$ , that is elliptically fibered with the same fiber as the original  $K3$ , which we call  $S$ .

In figure 4 we have depicted the polyhedra  $\nabla$  that defines  $\tilde{S}$  for the Calabi-Yau three-folds considered in section sections 5.1.1 and 5.1.3 respectively. The two polyhedra are obtained by projecting  $\nabla_{CY_3}$  given by (5.1) and (5.14) respectively, on the first, the third and the fourth coordinates.<sup>11</sup> The distribution of branes is very different in the two cases. Indeed, in the first case, the distribution of points above and below the polygon associated to the elliptic fiber gives two Dynkin diagrams that correspond to the trivial group. This is consistent with the fact that  $\xi$  in this case has zeros at generic points (i.e. they do not correspond to the North or the South pole) so no symmetry enhancement is expected. This picture is modified when we look at the Calabi-Yau three-fold considered in section 5.1.3. The points above and below the polygon are now associated to two  $SU(9)$  extended Dynkin diagrams. This is consistent with the expected gauge symmetry enhancement in the world volumes of colliding branes. The same results can be found from a careful analysis of the corresponding discriminants for the two choices of Calabi-Yau threefolds.

## 6 Other examples of auxiliary CY threefolds

In section 4 we presented a detailed analysis of the complex structure moduli space for a particular  $K3$  surface with two complex structure parameters. A similar analysis can be performed for any of the 9  $K3$  surfaces from the Kreuzer-Skarke list that have Picard number 18 and two complex structure parameters. These surfaces are defined in terms of polytopes which we present in appendix D.

In this section we summarise the results for two other  $K3$  surfaces and work out the geometry to flux dictionary derived from fibering these  $K3$  surfaces over  $S^2$ .

<sup>11</sup> $S$  is obtained by projecting  $\nabla_{CY_3}$  on the last three coordinates.

## 6.1 The second $K3$ surface

### 6.1.1 The moduli space

The defining pair of dual polyhedra  $(\nabla, \Delta)$  for this  $K3$  surface is given in (D.1) and (D.2). These polyhedra lead to the following polynomial:

$$f_{\text{hom}} = -c_0 z_1 z_2 z_3 z_4 + c_1 z_1^{12} + c_2 z_1^6 z_2^6 + c_3 z_2^{12} + c_4 z_3^3 + c_5 z_4^2 = 0 \quad (6.1)$$

This equation defines a  $K3$  hypersurface in  $\mathbb{CP}_{[1,1,4,6]}$ .

Including for later convenience numerical factors, the relevant combinations of coefficients which appear in the expansion for the fundamental period are

$$\xi = \frac{c_1 c_3 c_4^4 c_5^6}{c_0^{12}} \quad \text{and} \quad \eta = \frac{c_2 c_4^2 c_5^3}{c_0^6}. \quad (6.2)$$

The Frobenius period is given by

$$\varpi = \sum_{k,l=0}^{\infty} \frac{a_{k+\alpha, l+\beta}}{a_{\alpha, \beta}} \xi^{k+\alpha} \eta^{l+\beta}, \quad (6.3)$$

with

$$\begin{aligned} a_{k,l} &= \frac{\Gamma(12k + 6l + 1)}{\Gamma^2(k+1) \Gamma(l+1) \Gamma(4k + 2l + 1) \Gamma(6k + 3l + 1)} \\ &= 432^{2k+l} \frac{\Gamma(2k + l + \frac{1}{6}) \Gamma(2k + l + \frac{5}{6})}{\Gamma^2(k+1) \Gamma(l+1) \Gamma(2k + l + 1)} \end{aligned} \quad (6.4)$$

where the last equality has been obtained by using the multiplication formula for the  $\Gamma$ -function:

$$\Gamma(1 + mz) = (2\pi)^{-\frac{1}{2}(m-1)} m^{-\frac{1}{2}+mz} \prod_{r=1}^m \Gamma\left(z + \frac{r}{m}\right) \quad (6.5)$$

from which it follows immediately that

$$\frac{\Gamma(1 + m(z + \gamma))}{\Gamma(1 + m\gamma)} = m^{mz} \prod_{r=1}^m \frac{\Gamma(z + \gamma + \frac{r}{m})}{\Gamma(\gamma + \frac{r}{m})} \quad (6.6)$$

We find that the Picard-Fuchs equations are generated by the second order operators

$$\begin{aligned} \mathcal{L}_1 &= \theta_\eta (2\theta_\xi + \theta_\eta) - 432 \eta \left( 2\theta_\xi + \theta_\eta + \frac{5}{6} \right) \left( 2\theta_\xi + \theta_\eta + \frac{1}{6} \right), \\ \mathcal{L}_2 &= \eta^2 \theta_\xi^2 - \xi \theta_\eta (\theta_\eta - 1) \end{aligned} \quad (6.7)$$

The form of the second of these operators is non-standard. Applying Frobenius' method, we find three (instead of two) indicial equations, namely  $\alpha(\alpha - 2\beta) = 0$ ,  $\beta^2 = 0$  and  $\alpha(\alpha - 1) = 0$ . This is too restrictive. Indeed, the expansion of the Frobenius period in terms of  $\alpha$  and  $\beta$  has, in this case, only two terms corresponding to 1 and  $\beta$ . In order to rectify this situation, we perform the change of variables

$$u = \frac{\xi}{\eta^2} \quad v = \eta. \quad (6.8)$$

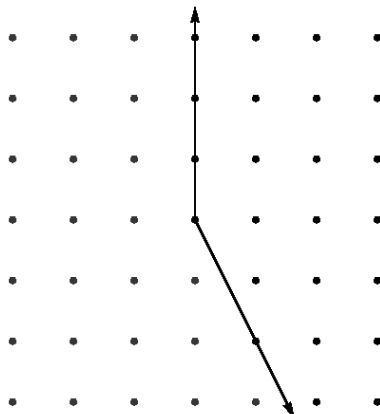


**Figure 5.** The cone of summation in  $(k, l)$ -space, corresponding to the first quadrant for the integers  $(m, n)$ . Note that  $\varpi_{0,0}$  itself restricts to the subcone  $k \geq 0, l \geq 0$  owing to the factor of  $\Gamma(n - 2m + 1)$  in the denominator of the coefficients  $b_{m,n}$  (see (6.10)). For the other periods, however, the summation corresponds to the points in the larger cone.

With this change of variables, the Frobenius period takes the form:

$$\varpi_{00}(u, v) = \sum_{m,n=0}^{\infty} \frac{b_{m+\epsilon, n+\delta}}{b_{\epsilon, \delta}} u^{m+\epsilon} v^{n+\delta}, \tag{6.9}$$

where

$$b_{m,n} = \frac{\Gamma(6n + 1)}{\Gamma^2(m + 1) \Gamma(n - 2m + 1) \Gamma(2n + 1) \Gamma(3n + 1)}. \tag{6.10}$$

A basis for the Picard-Fuchs operators is given by

$$\begin{aligned} \mathcal{L}_1 &= (\theta_v - 2\theta_u)\theta_v - 432v \left(\theta_v + \frac{1}{6}\right) \left(\theta_v + \frac{5}{6}\right), \\ \mathcal{L}_2 &= \theta_u^2 - u(\theta_v - 2\theta_u)(\theta_v - 2\theta_u - 1) \end{aligned} \tag{6.11}$$

Applying Frobenius' method to the above Picard-Fuchs operators, we find this time two indicial equations  $\epsilon(\epsilon - 2\delta) = 0$  and  $\delta^2 = 0$ , which lead to the following basis of periods

$$\begin{aligned} \varpi_0 &= \varpi_{00} = h_{00} \\ \varpi_1 &= \varpi_{10} + \varpi_{01} = \frac{1}{2\pi i} h_{00} \log(uv) + h_{10} + h_{01} \\ \varpi_2 &= \varpi_{01} = \frac{1}{2\pi i} h_{00} \log v + h_{01} \\ \varpi_3 &= \varpi_{11} + \varpi_{02} = \frac{1}{(2\pi i)^2} h_{00} \log(uv) \log v + h_{11} + h_{02} \end{aligned} \tag{6.12}$$

and  $\varpi_0 \varpi_3 = \varpi_1 \varpi_2$ . We identify the field combinations  $\sigma$  and  $\tau$  with the period ratios

$$\begin{aligned} \tau^{(1)} &= \frac{\varpi_{10}}{\varpi_{00}} = \frac{1}{2\pi i} \log(uv) + \frac{h_{10} + h_{01}}{h_{00}} \\ \tau^{(2)} &= \frac{\varpi_{01}}{\varpi_{00}} = \frac{1}{2\pi i} \log v + \frac{h_{01}}{h_{00}} \end{aligned} \tag{6.13}$$

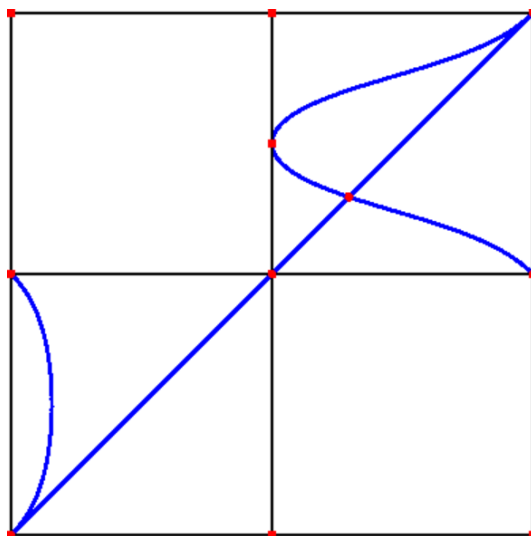


**Figure 6.** A sketch of the  $(u, v)$ -plane, where  $w = uv$ . The blue curves correspond to  $D = 0$  and  $1 - 4u = 0$ . The plane has been compactified to  $\mathbb{CP}^1 \times \mathbb{CP}^1$  so opposite boundaries on the plot, where  $u$  and  $v$  are infinite, should be identified.

	$v = 0$	$u = 0$
$uv j_1$	$\frac{1 + \sqrt{1 - 4u}}{2}$	$1 - 3 \cdot 12^2 v$
$v j_2$	$\frac{1 - \sqrt{1 - 4u}}{2u}$	$\frac{1}{(1 - 3 \cdot 12^2 v)}$

**Table 6.** The form of  $j_1$  and  $j_2$  along the curves  $u = 0$  and  $v = 0$ .

The associated  $j$ -functions satisfy

$$\begin{aligned}
 j_1 + j_2 &= \frac{1 - 3 \cdot 12^2 v + 12^3 uv}{uv} \\
 j_1 j_2 &= \frac{1}{uv^2}
 \end{aligned}
 \tag{6.14}$$

which, in turn, lead to:

$$j_{1,2} = \frac{1 - 3 \cdot 12^2 v + 12^3 vu \pm \sqrt{(1 - 4u)D}}{2uv},
 \tag{6.15}$$

where the discriminant locus, sketched in figure 6, is given by

$$D = (1 - 3 \cdot 12^2 v)^2 - 3 \cdot 12^5 uv^2.
 \tag{6.16}$$

In table 6 we collect the expressions that the  $j$ -functions take along the curves  $u = 0$  and  $v = 0$ . These limits are important for inferring the brane content of the supergravity solutions discussed below.

	$c_0, c_2$	$c_1, c_3$	$c_4$	$c_5$
$(q_1, q_2)$	$(0, 0)$	$(1, 0)$	$(3, 3)$	$(2, 2)$

**Table 7.** Branes of charge  $(q_1, q_2)$  are located at the zeros of  $c_a$ 's.

It is interesting that the last entry of the table corresponds to the following relation: if  $\tau$  and  $z$  are related by

$$\tau = i \frac{{}_2F_1\left(\frac{1}{6}, \frac{5}{6}; 1; 1-z\right)}{{}_2F_1\left(\frac{1}{6}, \frac{5}{6}; 1; z\right)}, \tag{6.17}$$

then

$$j(\tau) = \frac{432}{z(1-z)}. \tag{6.18}$$

### 6.1.2 Geometry to flux dictionary

Consider the four-dimensional polytope  $\nabla_{\text{CY}_3}$  obtained from the polyhedron (D.1) by adding two points in the fourth dimension, having vertices

$$w_i^{\text{CY}_3} = (0, w_i^{K3}), \quad w_5^{\text{CY}_3} = (-1, 0, 0, 0), \quad w_6^{\text{CY}_3} = (1, 0, 0, 0), \quad i = 1, \dots, 4 \tag{6.19}$$

The dual polytope contains 18 points. The defining polynomial is given by (6.1), with the coefficients replaced by homogenous polynomials of degree two in  $z = (z_5, z_6)$  parametrizing the  $\mathbb{CP}^1$  base:

$$f_{\text{CY}_3, \text{hom}} = -c_0(z) z_1 z_2 z_3 z_4 + c_1(z) z_1^{12} + c_2(z) z_1^6 z_2^6 + c_3(z) z_2^{12} + c_4(z) z_3^3 + c_5(z) z_4^2 \tag{6.20}$$

The period ratios are given by the above formulas with

$$u(z) = \frac{c_1(z) c_3(z)}{c_2(z)^2}, \quad v(z) = \frac{c_2(z) c_4(z)^2 c_5(z)^3}{c_0(z)^6}. \tag{6.21}$$

As in section 5, we can find the locations of branes by looking for the poles of  $j_1(z)$  and  $j_2(z)$ , which lie along the curves  $u = 0$  and  $v = 0$ . We find that both  $j_1$  and  $j_2$  degenerate at the zeros of  $c_4$  and  $c_5$  with poles of orders 2 and 3, respectively. Moreover,  $j_1$  has single poles at the zeros of  $c_1$  and  $c_3$ . The resulting brane content is summarised in the table 7. Taking into account that each  $c_a(z)$  has two zeros, one finds  $4 \times (0, 1) + 2 \times (3, 3) + 2(2, 2)$  for a total number of 24 branes, as required.

## 6.2 The third K3

### 6.2.1 The moduli space

The pair of polyhedra  $(\nabla, \Delta)$  defining this K3 surface is given in (D.5) and (D.6). These lead to the polynomial:

$$f = -c_0 z_1 z_2 z_3 z_4 z_5 + c_1 z_1^3 z_3^3 + c_2 z_1^3 z_4^3 + c_3 z_2^3 z_3^3 + c_4 z_2^3 z_4^3 + c_5 z_5^3 \tag{6.22}$$

defining a K3 hypersurface in the toric variety given by the weight system in table 8.

	$z_1$	$z_2$	$z_3$	$z_4$	$z_5$
$Q_1$	1	1	0	0	1
$Q_2$	0	0	1	1	1

**Table 8.** Weight system for the toric variety embedding the third  $K3$  surface.

The relevant invariant combinations of coefficients for this case are

$$\frac{\xi}{27} = \frac{c_1 c_4 c_5}{c_0^3} \quad \text{and} \quad \frac{\eta}{27} = \frac{c_2 c_3 c_5}{c_0^3} . \tag{6.23}$$

The fundamental period is given by

$$\begin{aligned} \varpi_{00}(\xi, \eta) &= \sum_{k,l=0}^{\infty} \frac{\Gamma(3k+3l+1)}{\Gamma(k+1)^2 \Gamma(l+1)^2 \Gamma(k+l+1)} \left(\frac{\xi}{27}\right)^k \left(\frac{\eta}{27}\right)^l \\ &= \sum_{k,l=0}^{\infty} a_{k,l} \left(\frac{\xi}{27}\right)^k \left(\frac{\eta}{27}\right)^l . \end{aligned} \tag{6.24}$$

We find the following second order operators that generate the Picard-Fuchs equations

$$\begin{aligned} \mathcal{L}_1 &= 9\theta_\xi^2 - \xi(3\theta_\xi + 3\theta_\eta + 1)(3\theta_\xi + 3\theta_\eta + 2) , \\ \mathcal{L}_2 &= 9\theta_\eta^2 - \eta(3\theta_\xi + 3\theta_\eta + 1)(3\theta_\xi + 3\theta_\eta + 2) . \end{aligned} \tag{6.25}$$

Applying Frobenius' method to the above Picard-Fuchs operators, we find two indicial equations, namely  $\epsilon^2 = 0$  and  $\delta^2 = 0$  and therefore a basis of periods

$$\begin{aligned} \varpi_{00} &= h_{00} \\ \varpi_{10} &= \frac{1}{2\pi i} h_{00} \log\left(\frac{\xi}{27}\right) + h_{10} \\ \varpi_{01} &= \frac{1}{2\pi i} h_{00} \log\left(\frac{\eta}{27}\right) + h_{01} \\ \varpi_{11} &= \frac{1}{(2\pi i)^2} h_{00} \log\left(\frac{\xi}{27}\right) \log\left(\frac{\eta}{27}\right) + h_{11} \end{aligned} \tag{6.26}$$

with  $\varpi_{00}\varpi_{11} = \varpi_{10}\varpi_{01}$ . We identify the field combinations  $\sigma$  and  $\tau$  with the period ratios

$$\begin{aligned} \tau^{(1)} &= \frac{\varpi_{10}}{\varpi_{00}} = \frac{1}{2\pi i} \log\left(\frac{\xi}{27}\right) + \frac{h_{10}}{h_{00}} \\ \tau^{(2)} &= \frac{\varpi_{01}}{\varpi_{00}} = \frac{1}{2\pi i} \log\left(\frac{\eta}{27}\right) + \frac{h_{01}}{h_{00}} \end{aligned} \tag{6.27}$$

The corresponding  $j_1 = j(\tau^{(1)})$  function takes the form:

$$j_1 = \frac{27}{2\eta^3\xi} \left[ 2\eta^3 - 486\eta\xi(-2\eta - 3\xi + 3) + Q \left( \sqrt{D} + \xi - \eta - 1 \right) \right] \tag{6.28}$$

where  $Q = (\eta - 9\xi)^3 - 243\xi(-2\eta - 6\xi + 3)$  and  $D$  is the discriminant:

$$D = (\eta - \xi)^2 - 2(\eta + \xi) + 1 . \tag{6.29}$$

	$\xi = 0$	$\eta = 0$
$\xi, j_1$	$27(1 - \eta)$	$\frac{27(1 + 8\xi)^3}{(1 - \xi)^3}$
$\eta, j_2$	$\frac{27(1 + 8\eta)^3}{(1 - \eta)^3}$	$27(1 - \xi)$

**Table 9.** The form of  $j_1$  and  $j_2$  along the curves  $\xi = 0$  and  $\eta = 0$ .

The expression for  $j_2 = j(\tau^{(2)})$  is analogous, and can be obtained from (6.28) by interchanging  $\xi$  and  $\eta$ .

In table 9 we have collected the expressions for  $j_1$  and  $j_2$  in the limits  $\xi \rightarrow 0$  and  $\eta \rightarrow 0$ . Remarkably, the expressions for  $j_1$  in the limit  $\eta \rightarrow 0$  and for  $j_2$  in the limit  $\xi \rightarrow 0$  correspond to the  $SL(2, \mathbb{Z})$ -invariants of two different tori. Accordingly,  $\tau^{(1)}(\xi, 0)$  and  $\tau^{(2)}(0, \eta)$  are given by

$$\tau^{(1)}(\xi, 0) = \tau^{(2)}(0, \eta) = \frac{i}{\sqrt{3}} \frac{{}_2F_1\left(\frac{1}{3}, \frac{2}{3}; 1; 1 - \xi\right)}{{}_2F_1\left(\frac{1}{3}, \frac{2}{3}; 1; \xi\right)}. \quad (6.30)$$

## 6.2.2 Geometry to flux dictionary

Consider the four-dimensional polytope  $\nabla_{\text{CY}_3}$  obtained from the polyhedron (D.5) by adding two points in the fourth dimension, above and respectively below the origin. The polytope thus constructed has vertices

$$w_i^{\text{CY}_3} = (0, w_i^{K^3}), \quad w_6^{\text{CY}_3} = (-1, 0, 0, 0), \quad w_7^{\text{CY}_3} = (1, 0, 0, 0), \quad i = 1, \dots, 5 \quad (6.31)$$

The dual polytope contains 18 points. The defining polynomial is given by (6.22) but with the  $c_a$  coefficients replaced by homogenous polynomials of order two in the two extra variables  $z = (z_6, z_7)$  spanning  $\mathbb{CP}^1$ :

$$f_{\text{CY}_3, \text{hom}} = -c_0(z) z_1 z_2 z_3 z_4 z_5 + c_1(z) z_1^3 z_3^3 + c_2(z) z_1^3 z_4^3 + c_3(z) z_2^3 z_3^3 + c_4(z) z_2^3 z_4^3 + c_5(z) z_5^3 \quad (6.32)$$

The period ratios  $\tau^{(i)}$  are given by the formulas in the last section with

$$\frac{\xi(z)}{27} = \frac{c_1(z) c_4(z) c_5(z)}{c_0(z)^3} \quad \text{and} \quad \frac{\eta(z)}{27} = \frac{c_2(z) c_3(z) c_5(z)}{c_0(z)^3}. \quad (6.33)$$

We notice that  $c_5(z)$  appears both in the definitions of  $\xi(z)$  and  $\eta(z)$ , so at the zeros of  $c_5$  both  $\xi$  and  $\eta$  vanish. To find the location of branes, we look for the poles of  $j_1(z)$  and  $j_2(z)$ . As before, the poles of  $j_1$  and  $j_2$  are located along the curves  $\xi = 0$  or  $\eta = 0$  and we can use the simpler formulas (6.27) to read off the monodromies. We find that  $\tau^{(1)}$  has a monodromy  $\tau^{(1)} \rightarrow \tau^{(1)} + 1$  around the zeros of  $c_1, c_4, c_5$  while  $\tau^{(2)}$  has a similar monodromy around the zeros of  $c_2, c_3, c_5$ . The brane content is summarised in the table 10.

Taking into account that each  $c_a(z)$  has two zeros, one finds  $4 \times (1, 0) + 4 \times (0, 1) + 2(1, 1) = 12$  branes. The intersection of the  $(\xi(z), \eta(z))$  curve with the discriminant locus

	$c_1, c_4$	$c_2, c_3$	$c_5$
$(q_1, q_2)$	$(1, 0)$	$(0, 1)$	$(1, 1)$

**Table 10.** Branes of charge  $(q_1, q_2)$  are located at the zeros of  $c_a$ 's.

$D = 0$  corresponds to 12 points in this example. Unlike in the previous examples, going around the locus  $D = 0$  leads to monodromies different from the  $\mathbb{Z}_2$  element that interchanges  $j_1$  and  $j_2$ . This suggests that 12 additional branes are located at the points of intersection between the curve  $(\xi(z), \eta(z))$  and the discriminant locus, leading to a total number of 24. However, the study of monodromies around these points is more involved.

## 7 Conclusions and outlook

Based on the ideas presented in [5, 6], in the present paper we studied the possibility of extending the F-theory approach to finding non-perturbative type IIB vacua with non-trivial fluxes. This approach was termed ‘G-theory’ in [5, 6]. While F-theory studies vacua with 7-branes and varying axio-dilaton field, G-theory aims to geometrize several other complex combinations of fluxes.

Concretely, we looked at type IIB solutions on  $\mathbb{R}^{1,3} \times T^4 \times S^2$  with the metric, the dilaton and the flux potentials varying over  $S^2$  and the flux potentials oriented along  $T^4$ . We started by finding local solutions on  $\mathbb{R}^{1,3} \times T^4 \times \mathbb{C}$  through a sequence of S and T dualities performed on a class of Ricci-flat geometries with trivial fluxes. These solutions are characterised by  $n \leq 3$  holomorphic functions that span the moduli space:

$$\mathcal{M}_{\text{BPS}} = \text{SO}(2, n, \mathbb{Z}) \setminus \frac{\text{SO}(2, n, \mathbb{R})}{\text{SO}(2, \mathbb{R}) \times \text{SO}(n, \mathbb{R})} \tag{7.1}$$

The main observation in G-theory is that this moduli space matches the moduli space of complex structures of a  $K3$  surface with Picard number  $20 - n$ . The flux solution can then be viewed as a fibration of an auxiliary  $K3$  fibered over  $S^2$ . The degeneration points of the  $K3$  fibration are associated to different types of branes, as indicated by the monodromies of the corresponding holomorphic combinations of flux fields.

In the present paper we focused mainly on the sub-class of solutions corresponding to  $n = 2, 3$ . For the  $n = 2$  case, we worked out in detail the map between the two holomorphic combinations of fluxes and the period ratios of the holomorphic two form describing the complex structure of the auxiliary  $K3$  surface. We inferred the brane content of the flux solutions from the  $\text{SO}(2, n, \mathbb{Z})$  monodromies of these functions around brane locations. In addition, the presence of a brane curves the base space (brane tension) generating a deficit angle of  $\pi/6$  [42], so a compact  $S^2$  arises for a total of 24 branes. As a consistency check, we showed that in each example considered this number is reproduced.

The results obtained here can be easily generalised. In fact, we have worked out the details of the flux-to-period map in a couple of other examples, summarised in section 6. We anticipate that a similar analysis can be performed for the local solutions involving



$n = 3$ ,  $n = 4$  and  $n = 5$  holomorphic functions, a task to which we hope to return in a future publication.

The techniques developed here can also be applied in contexts different from the one under consideration. Recently, in [55], non-geometric heterotic backgrounds with  $E_8 \times E_8$  and  $E_8 \times E_7$  vector bundles were studied by relating them to geometries based on  $K3$  surfaces admitting  $n = 2, 3$  complex deformations. The flux/geometry dictionary built here provides additional geometries that can be studied from the heterotic perspective. Conversely, the field/geometry dictionary built in [55] (see also [5, 6]) for  $K3$  surfaces with  $E_8 \times E_7$  singularities provides explicit realisations of flux solutions of class A, B and C characterised by  $n = 3$  holomorphic solutions. Finally, it would be nice to study the gauge duals of the supergravity solutions presented here. We observe that near the locations of branes, supergravity fields exhibit logarithmic divergences and an infinite tower of instanton corrections that can be tested against the dual gauge theory along the lines of [56].

### Acknowledgments

The authors would like to thank A. Braun, V. Braun, C. Hull, L. Martucci, M. Petrini and D. Waldram for interesting discussions and valuable comments. In addition, Volker Braun provided much assistance with the use of Sage. CD, ML and JFM would like to thank the Mathematical Institute, University of Oxford and Theoretical Physics group at Imperial College London for their kind hospitality during parts of this project. The work of PC is supported by EPSRC grant BKRWDM00. AC would like to thank the University of Oxford and the STFC for support during part of the preparation of this paper. The research of ML was supported by the Swedish Research Council (VR) under the contract 623-2011-7205. The work of JFM is supported by EPSRC, grant numbers EP/I01893X/1 and EP/K034456/1 and the ERC Advanced Grant n. 226455.

### A A brief review of toric geometry

In this section we review the notions of toric geometry needed in sections 4, 5 and 6.

Let  $M, N \cong \mathbb{Z}^p$  be two dual lattices. Let  $\Delta$  be a lattice polytope in  $M$ , i.e. a polytope realised as the convex hull of a finite number of points in  $M$ . The polytope  $\Delta$  is said to be reflexive if it contains the origin as its unique interior point and if the dual polytope  $\nabla \subset N \otimes \mathbb{R}$ , defined as

$$\nabla = \{w \in N \otimes \mathbb{R} \mid \langle v, w \rangle \geq -1, \text{ for all } v \in \Delta\} \tag{A.1}$$

is also a lattice polytope. An example of a pair of dual three-dimensional polytopes is given in figure 3.

Given a pair of reflexive polytopes  $(\Delta, \nabla)$ , one can construct a  $p$ -dimensional toric variety from the fan over a triangulation of the surface of  $\nabla$ , and a Calabi-Yau hypersurface in this toric variety as the zero locus of a polynomial whose monomials are in one-to-one correspondence with the lattice points of  $\Delta$ . This construction is described in the texts [57–60].

Following Cox’s approach, the toric variety can be constructed as an algebraic generalisation of complex weighted projective spaces. Concretely, let  $\{w_i | i = 1, \dots, q\} \subseteq (\nabla \setminus \{0\}) \cap N$ , be a subset of the lattice points of  $\nabla$  which includes its vertices and corresponds to a triangulation of its surface. In Cox’s approach, one assigns a homogeneous coordinate  $z_i \in \mathbb{C}^q$  to each vertex  $w_i$  of  $\nabla$ . After removing an exceptional set — in analogy to removing the origin of  $\mathbb{C}^{n+1}$  in the construction of  $\mathbb{C}P^n$  (see e.g. the texts [57–60] for details) — one identifies the points of  $\mathbb{C}^q$  using the certain equivalence relations. The equivalence relations are obtained from the  $q - p$  linear relations between the vectors  $\{w_i\}$ :

$$\sum_{i=1}^q Q_a^i w_i = 0 \quad \text{where } a = 1, \dots, q - p. \tag{A.2}$$

The coefficients  $Q_a^i$  are called weights and they form a so-called weight system  $\{Q_a\}$ . The equivalence relations between the homogeneous coordinates are, for each  $a$ , given by

$$(z_1, \dots, z_q) \sim (\lambda^{Q_a^1} z_1, \dots, \lambda^{Q_a^q} z_q) \quad \text{for any } \lambda \in \mathbb{C}^*. \tag{A.3}$$

A Calabi-Yau hypersurface is then defined as the zero locus of a polynomial, homogeneous under any of the relations (A.3), whose monomials are associated to the lattice points of  $\Delta$

$$f_{\text{hom}} = \sum_{v_a \in \Delta \cap M} c_a \prod_{i=1}^q z_i^{\langle w_i, v_a \rangle + 1}. \tag{A.4}$$

The auxiliary geometrical construction presented in the previous section involves a  $K3$  fibered over  $\mathbb{C}P^1$ . Such fibrations can be realised as Calabi-Yau threefolds, described in toric geometry by a pair  $(\Delta, \nabla) \subset M \times N$  of reflexive four-dimensional polytopes, for which  $N$  has a distinguished three-dimensional sub-lattice  $N_3$ , such that  $\nabla_3 = \nabla \cap N_3$  is a three-dimensional reflexive polytope. The sub-polytope  $\nabla_3$  is associated with the fiber and divides the polytope  $\nabla$  into two parts, a top and a bottom [61–63]. The fan corresponding to the base space, obtained by projecting the fan of the fibration along the linear space spanned by the sub-polytope  $\nabla_3$  defines a  $\mathbb{C}P^1$  space [64]. The above description is dual to having a distinguished one-dimensional sub-lattice  $M_1 \subset M$ , such that the projection of  $\Delta$  along  $M_1$  is  $\Delta_3 = (\nabla_3)^*$ , the dual of  $\nabla_3$  [60]. This dual description is commonly referred to as ‘a slice is dual to a projection’.

$K3$  surfaces that are elliptic fibrations will also appear in the subsequent discussion. The fibration structure can be seen at the level of polytopes in a manner completely analogous to the Calabi-Yau three-fold case, see figure 3 for an example. As before, the two-dimensional polytope  $\nabla_2$  corresponding to the elliptic fiber divides the  $K3$  polytope  $\nabla$  into two parts. It is interesting to note that in this case, the distributions of points above and below the  $\nabla_2$  define two affine Dynkin diagrams, which, in the ADE case correspond to the Kodaira degeneration type of the elliptic fiber over two distinguished points in the base space, say the North and the South poles. In F-theory, the corresponding Lie groups appear as gauge groups in the low-energy theory. A similar connection will emerge, in certain limits, in our discussion.

Finally, let us mention that the number of complex structure parameters of a  $K3$  surface can be computed from the combinatorial data of the defining pair of three-dimensional polytopes:

$$n = l(\Delta) - 4 - \sum_{\text{2-faces } \theta \subset \Delta} l^*(\theta) + \sum_{\text{edges } \theta \subset \Delta} l^*(\theta) l^*(\theta^*) \quad (\text{A.5})$$

where  $l(\Delta)$  denotes the number of integer points of the polyhedron  $\Delta$ ,  $l^*(\theta)$  denotes the number of integer points interior to a 2-face or to an edge, and  $\theta^*$  is the dual face to  $\theta$ . Note that edges (1-faces) are dual to edges and vertices (0-faces) are dual to 2-faces.

## B The $K3$ moduli space — A more detailed presentation

### B.1 The discriminant locus

The  $K3$  surface  $S$  is singular at the points where the defining polynomial as well as all its derivatives vanish simultaneously. These conditions are equivalent with the following set of equations<sup>12</sup>

$$z_j \frac{\partial f_{\text{hom}}}{\partial z_j} = 0 ; \quad j = 1, \dots, 6 \quad (\text{no sum}). \quad (\text{B.1})$$

Generically, the above system admits no solutions. However, for special choices of coefficients, defining a certain locus in the moduli space (the discriminant locus), the system admits solutions.

If we denote the monomials of  $f_{\text{hom}}$  (including the  $c_a$ -coefficients and the signs) by  $m_0, \dots, m_5$  then the above six conditions become

$$\begin{aligned} m_0 + 3m_1 + 2m_4 &= 0, & m_0 + 3m_1 + 2m_5 &= 0, \\ m_0 + 3m_2 + 2m_4 &= 0, & m_0 + 3m_2 + 2m_5 &= 0, \\ m_0 + 3m_3 + 2m_4 &= 0, & m_0 + 3m_3 + 2m_5 &= 0. \end{aligned} \quad (\text{B.2})$$

with the monomials  $m_i$  satisfying the relations

$$m_1 m_2 m_3 = -\frac{\xi}{27} m_0^3 \quad \text{and} \quad m_4 m_5 = \frac{\eta}{4} m_0^2. \quad (\text{B.3})$$

From (B.2), it is immediate that  $m_1 = m_2 = m_3$  and  $m_4 = m_5$ . Then, the equations (B.2) and (B.3) admit a solution only if  $\xi$  and  $\eta$  belong to the discriminant locus  $D = 0$  with

$$D = (\xi - 1 - 3\eta)^2 - \eta(\eta + 3)^2. \quad (\text{B.4})$$

---

<sup>12</sup>The equation  $f_{\text{him}} = 0$  is recovered by summing up the l.h.s. of the equations in (B.1) and equating this with 0.

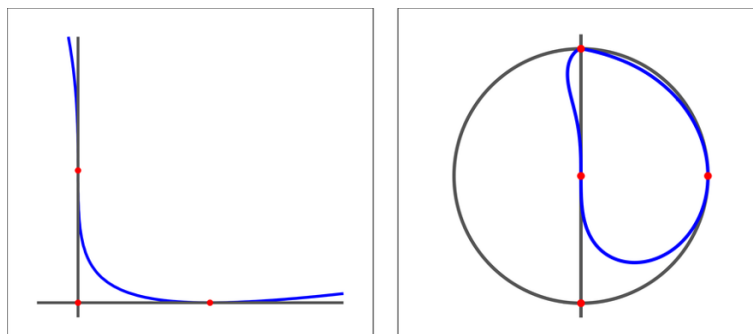


**Figure 7.** On the left: the discriminant locus (in blue) showing also the curves  $\xi = 0$  and  $\eta = 0$ . The intersections with  $D$  are the points  $(1, 0)$  and  $(0, 1)$ . The locus  $D(\xi, \eta) = 0$  contains an extra isolated point in the real plane,  $(\xi, \eta) = (-8, -3)$ , not included in the plot. On the right, the upper half plane has been mapped to the unit disk in order to show the intersection at infinity.

**B.2 The period computation: PF equations and the method of Frobenius**

In section 4.2.2 we found the Picard-Fuchs operators

$$\begin{aligned} \mathcal{L}_1 &= 4\theta_\eta^2 - \eta(3\theta_\xi + 2\theta_\eta + 2)(3\theta_\xi + 2\theta_\eta + 1), \\ \mathcal{L}_2 &= 3\theta_\xi(3\theta_\xi - 2\theta_\eta) - \xi(3\theta_\xi + 2\theta_\eta + 2)(3\theta_\xi + 2\theta_\eta + 1) + 3\eta\theta_\xi(3\theta_\xi + 2\theta_\eta + 1). \end{aligned} \tag{B.5}$$

by searching for linear relations with polynomial coefficients among the elements of the set

$$\{\theta_\xi^i \theta_\eta^j \varpi_{00}\}_{0 \leq i+j \leq 2}. \tag{B.6}$$

Alternatively, the first operator  $\mathcal{L}_1$  may also be found from the recurrence relation

$$4(l+1)^2 a_{k,l+1} = (3k+2l+2)(3k+2l+1)a_{k,l} \tag{B.7}$$

satisfied by the expansion coefficients  $a_{k,l}$  in the series (4.5) for  $\varpi_{00}$ . A second recurrence relation

$$27(k+1)^3 a_{k+1,l} = (3k+2l+3)(3k+2l+2)(3k+2l+1)a_{k,l} \tag{B.8}$$

leads to the third order operator

$$\tilde{\mathcal{L}}_2 = 27\theta_\xi^3 - \xi(3\theta_\xi + 2\theta_\eta + 3)(3\theta_\xi + 2\theta_\eta + 2)(3\theta_\xi + 2\theta_\eta + 1). \tag{B.9}$$

In this alternative approach (see [65] for more details), the second order operator  $\mathcal{L}_2$  can be found by considering combinations of these two operators of the form  $\mathcal{M}\mathcal{L}_1 + B\tilde{\mathcal{L}}_2$ , where  $\mathcal{M}$  is a first order operator and  $B$  is a polynomial, and to seek to factor this operator into the product of a first order and a second order operator.

We believe, as indicated above, that the differential equations corresponding to these operators should admit four linearly independent solutions. To find these we have recourse to the method of Frobenius. Consider a quantity to which we will refer as the Frobenius period

$$\varpi = \sum_{k,l=0}^{\infty} a_{k,l}(\epsilon, \delta) \left(\frac{\xi}{27}\right)^{k+\epsilon} \left(\frac{\eta}{4}\right)^{l+\delta} \tag{B.10}$$

where the coefficients  $a_{k,l}$  now depend on  $\epsilon$  and  $\delta$ . We will suppress the arguments  $(\epsilon, \delta)$  below. Requiring that the Frobenius period is a solution of the differential equations associated with  $\mathcal{L}_1$  and  $\mathcal{L}_2$  results in certain constraints on the coefficients  $a_{k,l}$  and the exponents  $\epsilon$  and  $\delta$ . More precisely, acting with  $\mathcal{L}_1$  and, respectively,  $\mathcal{L}_2$  on  $\varpi$  produces two series with terms given by:

$$\begin{aligned}
 (\mathcal{L}_1 \varpi)_{k,l} &= \left[ 4(l + \delta)^2 a_{k,l} - 4 \left( 3(k + \epsilon) + 2(l + \delta - 1) + 2 \right) \times \right. \\
 &\quad \left. \times \left( 3(k + \epsilon) + 2(l + \delta - 1) + 1 \right) a_{k,l-1} \right] \left( \frac{\xi}{27} \right)^{k+\epsilon} \left( \frac{\eta}{4} \right)^{l+\delta} \\
 (\mathcal{L}_2 \varpi)_{k,l} &= \left[ 3(k + \epsilon) \left( 3(k + \epsilon) - 2(l + \delta) \right) a_{k,l} \right. \\
 &\quad \left. - 27 \left( 3(k + \epsilon - 1) + 2(l + \delta) + 2 \right) \left( 3(k + \epsilon - 1) + 2(l + \delta) + 1 \right) a_{k-1,l} \right. \\
 &\quad \left. + 12 \left( k + \epsilon \right) \left( 3(k + \epsilon) + 2(l + \delta - 1) + 1 \right) a_{k,l-1} \right] \left( \frac{\xi}{27} \right)^{k+\epsilon} \left( \frac{\eta}{4} \right)^{l+\delta}
 \end{aligned}$$

where the coefficients  $a_{k,l}$  are understood to vanish if at least one of the indices is negative.

If we choose the initial conditions  $a_{0,0} = 1$  then,  $\mathcal{L}_1 \varpi = \mathcal{L}_2 \varpi = 0$  implies

$$a_{k,l} = \frac{\Gamma^3(\epsilon + 1) \Gamma^2(\delta + 1)}{\Gamma(3\epsilon + 2\delta + 1)} \frac{\Gamma(3k + 3\epsilon + 2l + 2\delta + 1)}{\Gamma^3(k + \epsilon + 1) \Gamma^2(l + \delta + 1)}. \quad (\text{B.11})$$

The coefficients  $a_{k,l}$  reduce to those of (4.6) when  $\epsilon = \delta = 0$ . It is of interest to note also that the coefficients can be expressed simply in terms of Pochhammer symbols.<sup>13</sup> In terms of these symbols the coefficients may be written as

$$a_{k,l} = \frac{(3\epsilon + 2\delta + 1)_{3k+2l}}{(\epsilon + 1)_k^3 (\delta + 1)_l^3}. \quad (\text{B.12})$$

This has the consequence that, despite the initial appearance of (B.11), all the quantities

$$a_{k,l}^{(r,s)} = \left( \frac{\partial}{\partial \epsilon} \right)^r \left( \frac{\partial}{\partial \delta} \right)^s a_{k,l} \Big|_{\epsilon, \delta=0}, \quad (\text{B.13})$$

that we shall require shortly, are rational numbers.

Furthermore, the  $k = l = 0$  terms of the equations  $\mathcal{L}_1 \varpi = \mathcal{L}_2 \varpi = 0$  have to be treated separately. These imply the following relations

$$\delta^2 = 0, \quad \epsilon(3\epsilon - 2\delta) = 0. \quad (\text{B.14})$$

<sup>13</sup>The Pochhammer symbol  $(\zeta)_n$  is defined, for  $n = 0, 1, 2, \dots$ , by

$$(\zeta)_n = \frac{\Gamma(\zeta + n)}{\Gamma(\zeta)}.$$

Thus

$$(\zeta)_0 = 1, \quad (\zeta)_1 = \zeta \quad \text{and} \quad (\zeta)_n = \zeta(\zeta + 1) \cdots (\zeta + n - 1),$$

so  $(\zeta)_n$  is a polynomial in  $\zeta$  of degree  $n$ .

Multiplying the second of these relations by  $\delta$  and  $\epsilon$ , in turn, we learn that  $\epsilon^2\delta = 0$  and  $\epsilon^3 = 0$ . Thus all the cubic, and higher, monomials in  $\epsilon$  and  $\delta$  vanish.

We write

$$\varpi_{rs} = \frac{1}{(2\pi i)^{r+s}} \left( \frac{\partial}{\partial \epsilon} \right)^r \left( \frac{\partial}{\partial \delta} \right)^s \varpi \Big|_{\epsilon, \delta=0} \quad (\text{B.15})$$

and expand  $\varpi$  in terms of  $\epsilon$  and  $\delta$ , taking account of the relations (B.14),

$$\varpi = \varpi_{00} + 2\pi i \epsilon \varpi_{10} + 2\pi i \delta \varpi_{01} + (2\pi i)^2 \epsilon \delta \left( \varpi_{11} + \frac{1}{3} \varpi_{20} \right). \quad (\text{B.16})$$

The four functions identified by this expansion  $\{\varpi_{00}, \varpi_{10}, \varpi_{01}, 3\varpi_{11} + \varpi_{20}\}$  form a basis for the periods. If we define also the power series  $h_{rs}$  by

$$h_{rs} = \frac{1}{(2\pi i)^{r+s}} \sum_{k,l=0}^{\infty} a_{k,l}^{(r,s)} \left( \frac{\xi}{27} \right)^k \left( \frac{\eta}{4} \right)^l, \quad (\text{B.17})$$

then, writing  $\varpi_3$  for the combination  $3\varpi_{11} + \varpi_{20}$ , we have the relations

$$\begin{aligned} \varpi_{00} &= h_{00} \\ \varpi_{10} &= \frac{1}{2\pi i} h_{00} \log \left( \frac{\xi}{27} \right) + h_{10} \\ \varpi_{01} &= \frac{1}{2\pi i} h_{00} \log \left( \frac{\eta}{4} \right) + h_{01} \\ \varpi_3 &= \frac{1}{(2\pi i)^2} h_{00} \log \left( \frac{\xi}{27} \right) \log \left( \frac{\xi \eta^3}{1728} \right) + \frac{1}{2\pi i} (2h_{10} + 3h_{01}) \log \left( \frac{\xi}{27} \right) \\ &\quad + \frac{3}{2\pi i} h_{10} \log \left( \frac{\eta}{4} \right) + (3h_{11} + h_{20}). \end{aligned} \quad (\text{B.18})$$

The factors of  $2\pi i$  are chosen so that the monodromy matrices, that describe how the periods change as the singular loci  $\xi = 0$  and  $\eta = 0$  are encircled, are integral:

$$T_\xi = \begin{pmatrix} 1 & 0 & 0 & 0 \\ 1 & 1 & 0 & 0 \\ 0 & 0 & 1 & 0 \\ 1 & 2 & 3 & 1 \end{pmatrix}, \quad T_\eta = \begin{pmatrix} 1 & 0 & 0 & 0 \\ 0 & 1 & 0 & 0 \\ 1 & 0 & 1 & 0 \\ 1 & 3 & 0 & 1 \end{pmatrix}. \quad (\text{B.19})$$

Note that, if we write  $T_\xi = \mathbb{1} + R_\xi$  and  $T_\eta = \mathbb{1} + R_\eta$ , then the matrices  $R_\xi$  and  $R_\eta$  have the same algebra as  $\epsilon$  and  $\delta$ , namely:

$$R_\xi R_\eta = R_\eta R_\xi, \quad R_\eta^2 = 0, \quad 3R_\xi^2 = 2R_\xi R_\eta. \quad (\text{B.20})$$

This  $K3$  surface has Picard number 18 and so we expect the periods to factorise and be related to  $j$ -invariants. In order to see this factorisation let us return to the generators of the ideal (B.14). Modulo  $\delta^2$ , we may write the first generator as  $(\epsilon - \frac{1}{3}\delta)^2$  so setting  $\tilde{\epsilon} = \epsilon - \frac{1}{3}\delta$  we may write the generators in the more symmetric form

$$\tilde{\epsilon}^2 = 0 \quad \text{and} \quad \delta^2 = 0. \quad (\text{B.21})$$

Writing  $\epsilon$  in terms of  $\tilde{\epsilon}$  and  $\delta$ , we have  $\xi^\epsilon \eta^\delta = \xi^{\tilde{\epsilon}} (\eta \xi^{\frac{1}{3}})^\delta$ , suggesting that we should take as the natural coordinates  $\xi$  and  $\tilde{\eta} = \eta \xi^{\frac{1}{3}}$ . Note that by setting  $\varpi_0 = \varpi_{00}$ ,  $\varpi_1 = \varpi_{10}$ ,  $\varpi_2 = 3\varpi_{01} + \varpi_{10}$  and  $\varpi_3$  as before, we may take a slightly different basis to (B.18)

$$\begin{aligned} \varpi_0 &= \phi_0 \\ \varpi_1 &= \frac{1}{2\pi i} \phi_0 \log\left(\frac{\xi}{27}\right) + \phi_1 \\ \varpi_2 &= \frac{1}{2\pi i} \phi_0 \log\left(\frac{\xi \eta^3}{1728}\right) + \phi_2 \\ \varpi_3 &= \frac{1}{(2\pi i)^2} \phi_0 \log\left(\frac{\xi}{27}\right) \log\left(\frac{\xi \eta^3}{1728}\right) + \frac{1}{2\pi i} \phi_2 \log\left(\frac{\xi}{27}\right) + \frac{1}{2\pi i} \phi_1 \log\left(\frac{\xi \eta^3}{1728}\right) + \phi_3, \end{aligned} \tag{B.22}$$

where

$$\phi_0 = h_{00}, \quad \phi_1 = h_{10}, \quad \phi_2 = 3h_{01} + h_{10} \quad \text{and} \quad \phi_3 = 3h_{11} + h_{20}. \tag{B.23}$$

Note that

$$\varpi_3 = \frac{\varpi_1 \varpi_2}{\varpi_0} \quad \text{if} \quad \phi_1 \phi_2 = \phi_0 \phi_3. \tag{B.24}$$

The latter relation does indeed hold as can be checked by multiplication of the respective series. Thus if we write

$$\tau_1 = \frac{\varpi_1}{\varpi_0} \quad \text{and} \quad \tau_2 = \frac{\varpi_2}{\varpi_0} \quad \text{then} \quad \tau_1 \tau_2 = \frac{\varpi_3}{\varpi_0}. \tag{B.25}$$

## C Elliptic fibration structures

Elliptic fibration structures for the auxiliary  $K3$  surface proved to be important for establishing a link to F-theory, as discussed in section 5.2. In this appendix we present the 5 different fibration structures that can be torically described for the  $K3$  surface discussed in section 4. The first fibration structure already appeared in section 5.2.

We will present the three-dimensional polytope  $\nabla$  and the 5 different two-dimensional sub-polytopes contained in it as ‘slices’ (see the discussion in appendix A). In each case, we draw the corresponding extended Dynkin diagrams, which indicate the degeneration type of the elliptic fiber at  $z = 0$  and  $z = \infty$ .

## D $K3$ surfaces with Picard number 18 and two complex structures

**The second  $K3$ .** The polyhedron  $\nabla$  has 4 vertices:

$$w_i = \{(6, 2, 3), (-6, 2, 3), (0, -1, 0), (0, 0, -1)\}. \tag{D.1}$$

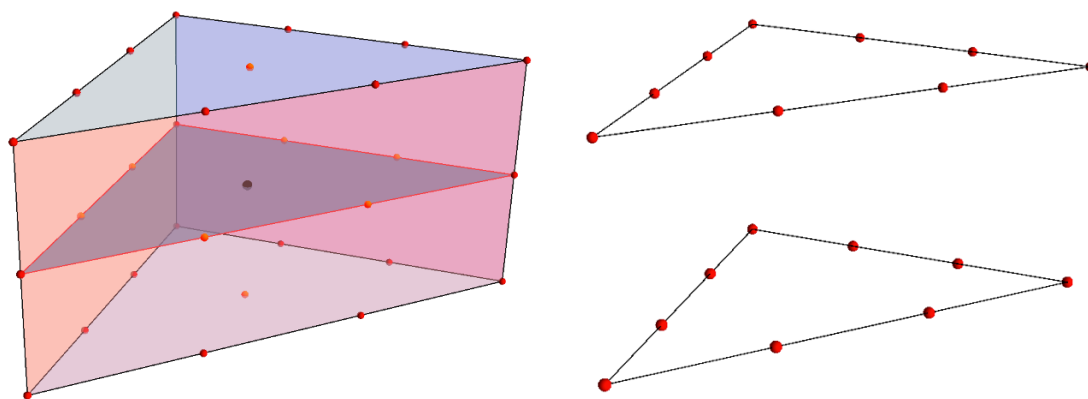


**Figure 8.** The first fibration structure. The Dynkin diagrams correspond to  $(SU(9), SU(9))$ .

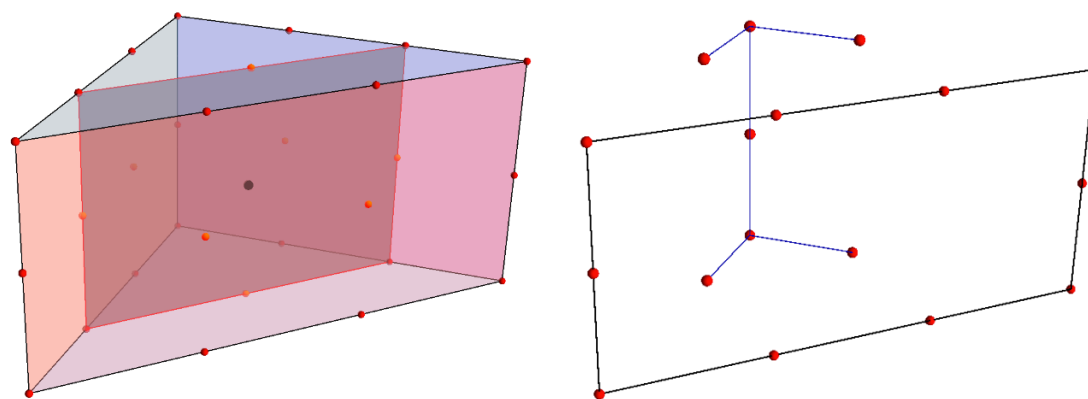


**Figure 9.** The second fibration structure. The Dynkin diagrams correspond to  $(SO(12), SU(10))$ .

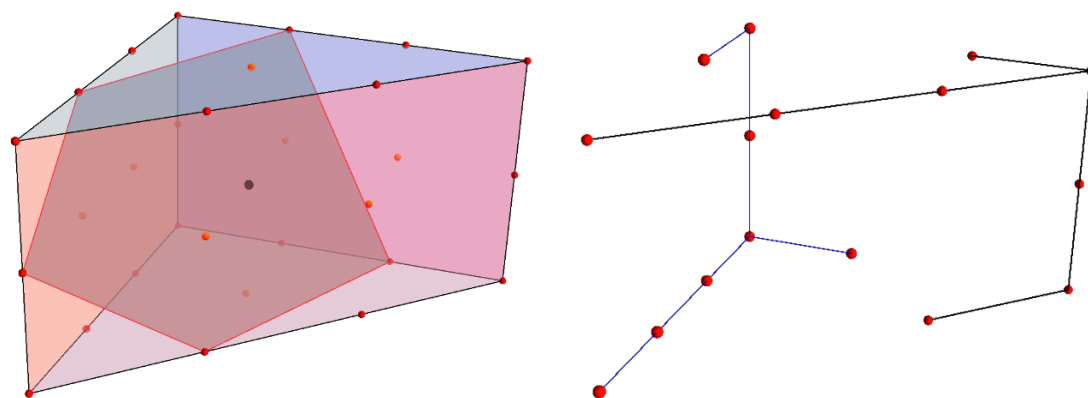


**Figure 10.** The third fibration structure. The Dynkin diagrams correspond to  $(E_7, E_7)$ .



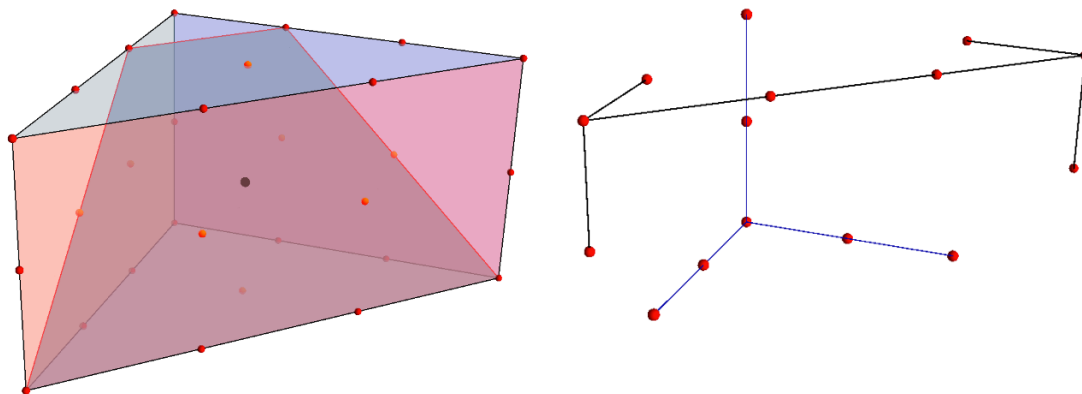


**Figure 11.** The fourth fibration structure. The Dynkin diagrams correspond to  $(SO(14), E_6)$ .

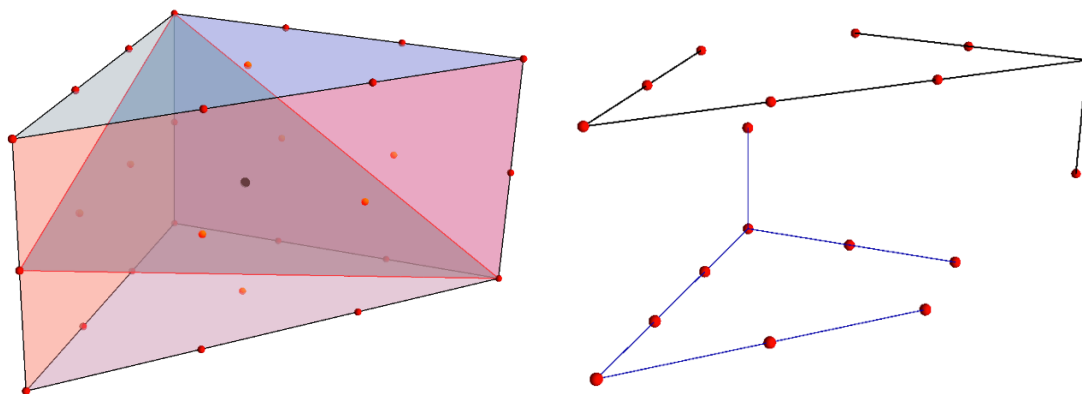


**Figure 12.** The fifth fibration structure. The Dynkin diagrams correspond to  $(E_8, E_8)$ .

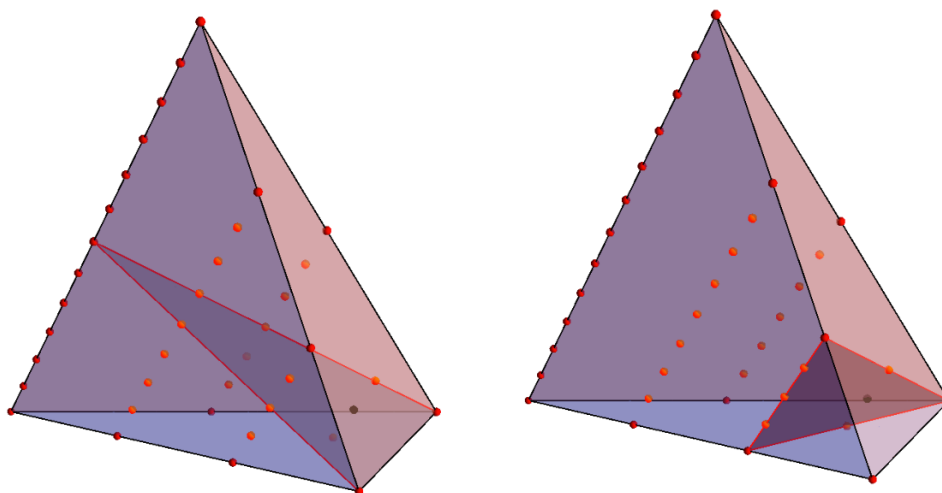


**Figure 13.** The second  $K3$  surface. Both polyhedra correspond to  $\nabla$  and indicate two different elliptic fibration structures, of types  $E_8 \times E_8$  and  $SO(32) \times \{1\}$ .

This  $K3$  admits two fibration structures, as indicated in figure 13. The first fibration structure is of type  $(E_8, E_8)$ , while the second one is of type  $(SO(32), \{1\})$ , where  $\{1\}$  denotes the trivial Lie group. This manifold appeared in earlier works, such as [61, 62].

The dual polyhedron  $\Delta$  has 9 points in total, and 4 vertices:

$$v_a = \{(-1, 1, 1), (1, 1, 1), (0, 1, -1), (0, -2, 1)\} . \quad (D.2)$$

Denoting by  $z_1, z_2, z_3, z_4$  the homogeneous coordinates associated with the vertices of  $\nabla$ , in the order given in eq. (D.1), we obtain the following polynomial:

$$f = -c_0 z_1 z_2 z_3 z_4 + c_1 z_1^{12} + c_2 z_1^6 z_2^6 + c_3 z_2^{12} + c_4 z_3^3 + c_5 z_4^2 + c_6 z_1^4 z_2^4 z_3 + c_7 z_1^2 z_2^2 z_3^2 + c_8 z_1^3 z_2^3 z_4 . \quad (D.3)$$

The monomials associated to points which are interior to the facets of  $\Delta$  can be removed by a suitable change of coordinates, such that  $c_6 = c_7 = c_8 = 0$ , leaving a polynomial of generic form

$$f = -c_0 z_1 z_2 z_3 z_4 + c_1 z_1^{12} + c_2 z_1^6 z_2^6 + c_3 z_2^{12} + c_4 z_3^3 + c_5 z_4^2 . \quad (D.4)$$

**The third  $K3$ .** The third  $K3$  surface is given by the polyhedron  $\nabla$  with vertices

$$w_i = \{(-1, -1, 2), (-1, 2, -1), (-1, 2, 2), (-1, -1, -1), (2, -1, -1)\} \quad (D.5)$$

and its dual  $\Delta$ , with vertices

$$v_a = \{(0, 0, 1), (-1, -1, 0), (1, 0, 0), (-1, 0, -1), (0, 1, 0)\} . \quad (D.6)$$

This pair of polyhedra leads to the following defining polynomial:

$$f = -c_0 z_1 z_2 z_3 z_4 z_5 + c_1 z_1^3 z_3^3 + c_2 z_1^3 z_4^3 + c_3 z_2^3 z_3^3 + c_4 z_2^3 z_4^3 + c_5 z_5^3 \quad (D.7)$$

The manifold admits 5 different elliptic fibration structures, depicted below.

**The fourth  $K3$ .** The fourth  $K3$  surface is given by a polyhedron  $\nabla$  with vertices

$$w_i = \{(-1, -1, -1), (0, -1, 2), (-1, 4, -1), (1, 0, -1), (-1, -1, 4), (0, -1, -1)\} \quad (D.8)$$

and its dual  $\Delta$ , with vertices

$$v_a = \{(-2, -1, -1), (-1, 1, 0), (0, 1, 0), (1, 0, 0), (0, 0, 1)\} . \quad (D.9)$$

Disregarding the points interior to the facets of  $\Delta$ , we obtain the following defining polynomial:

$$f = -c_0 z_1 z_2 z_3 z_4 z_5 z_6 + c_1 z_1^5 z_6^3 + c_2 z_2^3 z_5^5 + c_3 z_3^5 z_4 + c_4 z_1 z_3^6 z_5 + c_5 z_2 z_4^2 z_6 \quad (D.10)$$

This  $K3$  surface admits 4 different elliptic fibration structures.

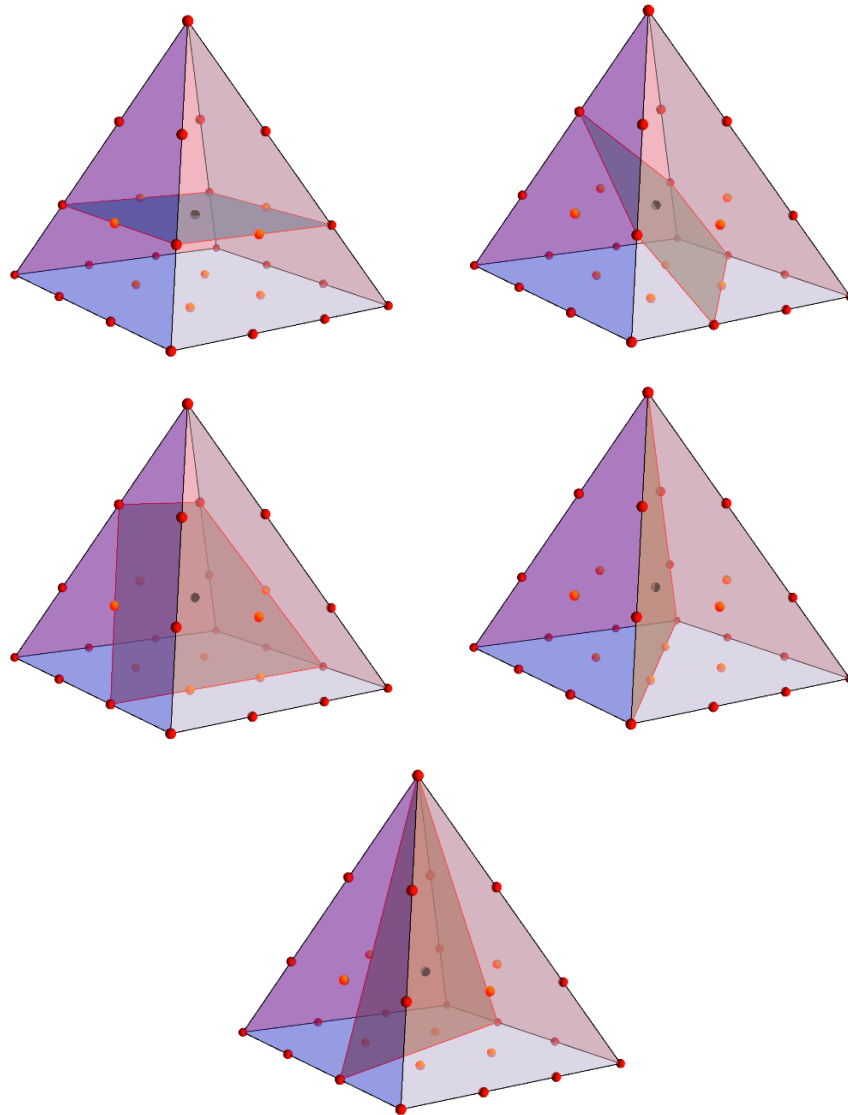


**Figure 14.** The polyhedron  $\nabla$  for the fifth  $K3$  surface. This  $K3$  admits five different elliptic fibration structures, of types  $SO(8) \times SU(12)$ ,  $SO(14) \times E_7$ ,  $SU(10) \times SO(14)$ ,  $E_6 \times E_6$  and  $E_8 \times E_8$ , from top left to bottom.

**The fifth  $K3$ .** The fifth  $K3$  surface is given by the polyhedron  $\nabla$  with vertices

$$w_i = \{(-1, -1, 1), (-1, -1, -1), (-1, 1, -1), (1, -1, 3), (1, -1, -1), (1, 3, -1)\} \tag{D.11}$$

and its dual  $\Delta$ , with vertices

$$v_a = \{(-1, 0, 0), (0, 0, 1), (0, 1, 0), (1, 0, 0), (1, -1, -1)\} . \tag{D.12}$$

The pair of dual polyhedra  $(\nabla, \Delta)$  leads, in this case, to the following defining polynomial:

$$f = -c_0 z_1 z_2 z_3 z_4 z_5 z_6 + c_1 z_1^2 z_4^4 + c_2 z_2^2 z_5^4 + c_3 z_3^2 z_6^4 + c_4 z_1^2 z_2^2 z_3^2 + c_5 z_4^2 z_5^2 z_6^2 \tag{D.13}$$

This  $K3$  surface admits 6 different elliptic fibration structures.

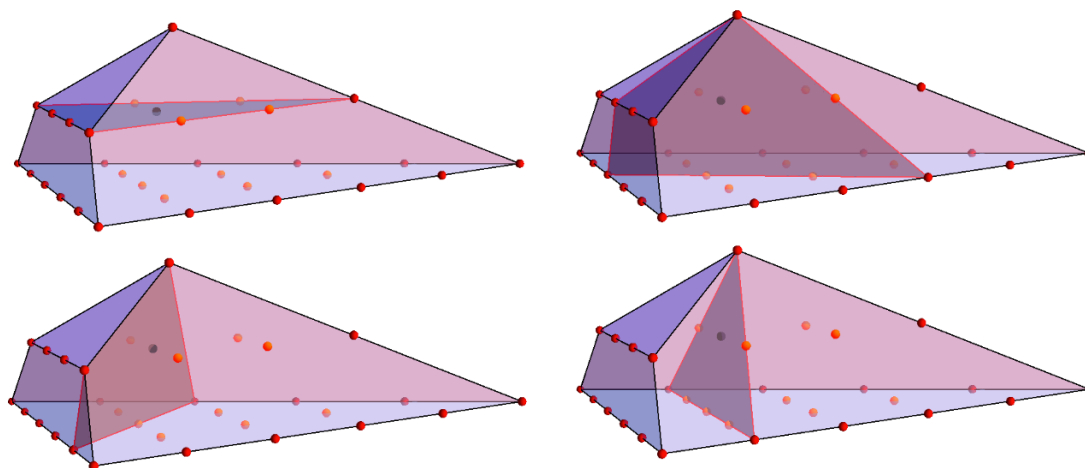


**Figure 15.** The polyhedron  $\nabla$  for the third  $K3$  surface. This  $K3$  admits four different elliptic fibration structures, of types  $\{1\} \times \text{SU}(15)$ ,  $E_6 \times \text{SO}(18)$ ,  $E_7 \times E_8$  and  $E_7 \times \text{SU}(10)$ , from top left to bottom right.

**The sixth  $K3$ .** The sixth  $K3$  surface is given by the polyhedron  $\nabla$  with vertices

$$w_i = \{(-1, -1, 0), (-1, -1, -1), (-1, 2, 0), (-1, 2, -1), (2, -1, 3), (2, -1, -1)\} \quad (\text{D.14})$$

and its dual  $\Delta$ , with vertices

$$v_a = \{(-1, -1, 0), (0, 1, 0), (1, 0, -1), (1, 0, 0), (0, 0, 1)\} . \quad (\text{D.15})$$

The pair of dual polyhedra  $(\nabla, \Delta)$  leads, in this case, to the following defining polynomial:

$$f = -c_0 z_1 z_2 z_3 z_4 z_5 z_6 + c_1 z_1^3 z_2^3 + c_2 z_3^3 z_4^3 + c_3 z_5^3 z_6^3 + c_4 z_1 z_3 z_5^4 + c_5 z_2 z_4 z_6^4 \quad (\text{D.16})$$

This manifold admits 7 different elliptic fibration structures, as displayed below.

**The seventh  $K3$ .** The seventh  $K3$  surface is given by a polyhedron  $\nabla$  with vertices

$$w_i = \{(-1, -1, 0), (-1, 0, -1), (-1, -1, -1), (1, -1, 4), (1, 4, -1), (1, -1, -1)\} \quad (\text{D.17})$$

and its dual  $\Delta$ , with vertices

$$v_a = \{(-1, 0, 0), (0, 0, 1), (0, 1, 0), (2, -1, -1), (1, 0, 0)\} . \quad (\text{D.18})$$

The pair  $(\nabla, \Delta)$  leads, in this case, to the following defining polynomial:

$$f = -c_0 z_1 z_2 z_3 z_4 z_5 z_6 + c_1 z_1 z_4^5 + c_2 z_2 z_5^5 + c_3 z_3 z_6^5 + c_4 z_1^2 z_2^2 z_3^2 + c_5 z_4^2 z_5^2 z_6^2 \quad (\text{D.19})$$

This  $K3$  surface admits 4 different elliptic fibration structures.

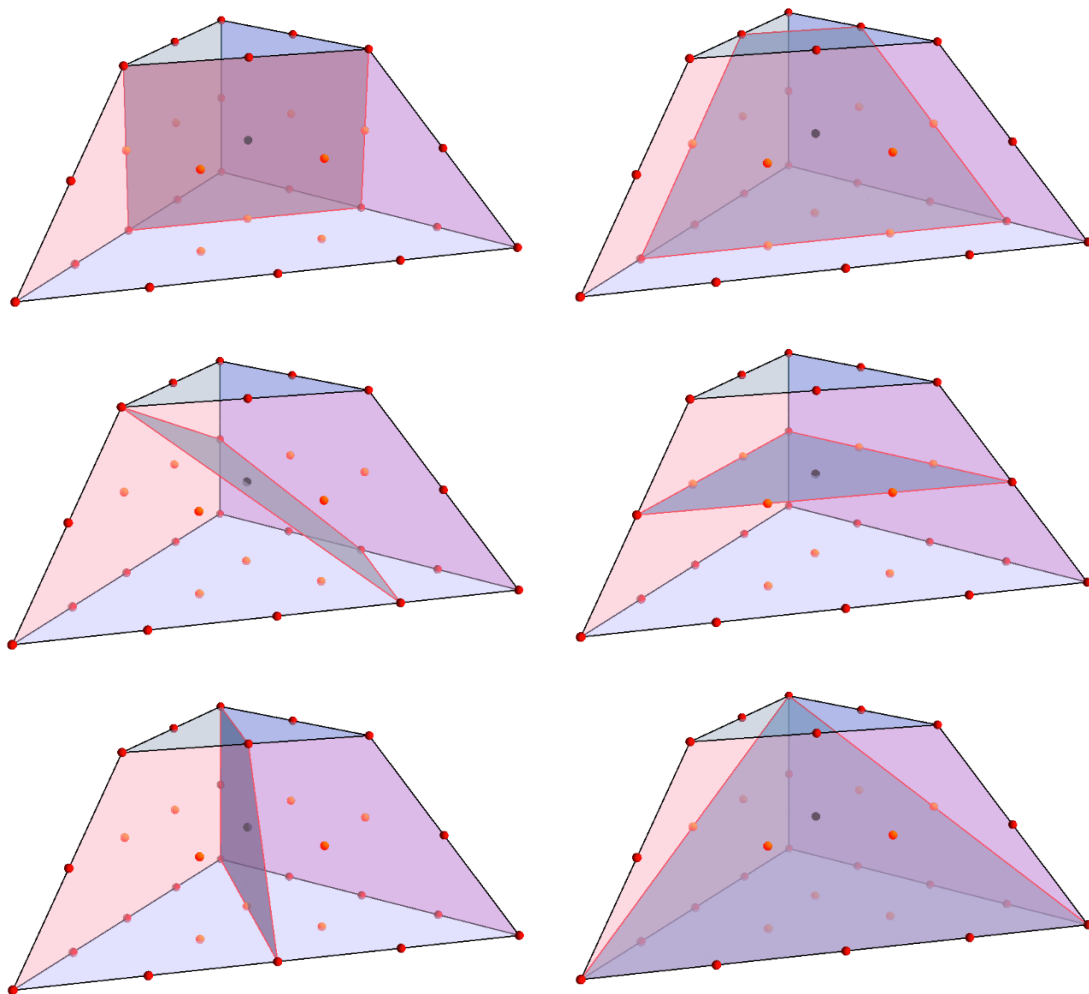


**Figure 16.** The polyhedron  $\nabla$  for the fourth  $K3$  surface. This  $K3$  admits six different elliptic fibration structures, of types  $SO(16) \times SO(12)$ ,  $E_6 \times SO(10)$ ,  $E_8 \times E_7$ ,  $SU(12) \times SU(6)$ ,  $E_7 \times E_7$  and  $E_7 \times SO(12)$ , from top left to bottom right.

**The eighth  $K3$ .** The eighth  $K3$  surface is given by a polyhedron  $\nabla$  with vertices

$$w_i = \{(-1, -1, -1), (-1, 3, 3), (1, -1, -1), (-1, -1, 3), (-1, 3, -1)\} \quad (D.20)$$

and its dual  $\Delta$ , with vertices

$$v_a = \{(-2, -1, 0), (-2, 0, -1), (0, 0, 1), (0, 1, 0), (1, 0, 0)\}. \quad (D.21)$$

The pair  $(\nabla, \Delta)$  leads, in this case, to the following defining polynomial:

$$f = -c_0 z_1 z_2 z_3 z_4 z_5 + c_1 z_1^4 z_4^4 + c_2 z_1^4 z_5^4 + c_3 z_2^4 z_4^4 + c_4 z_2^4 z_5^4 + c_5 z_3^2 \quad (D.22)$$

This  $K3$  surface admits 3 different elliptic fibration structures.

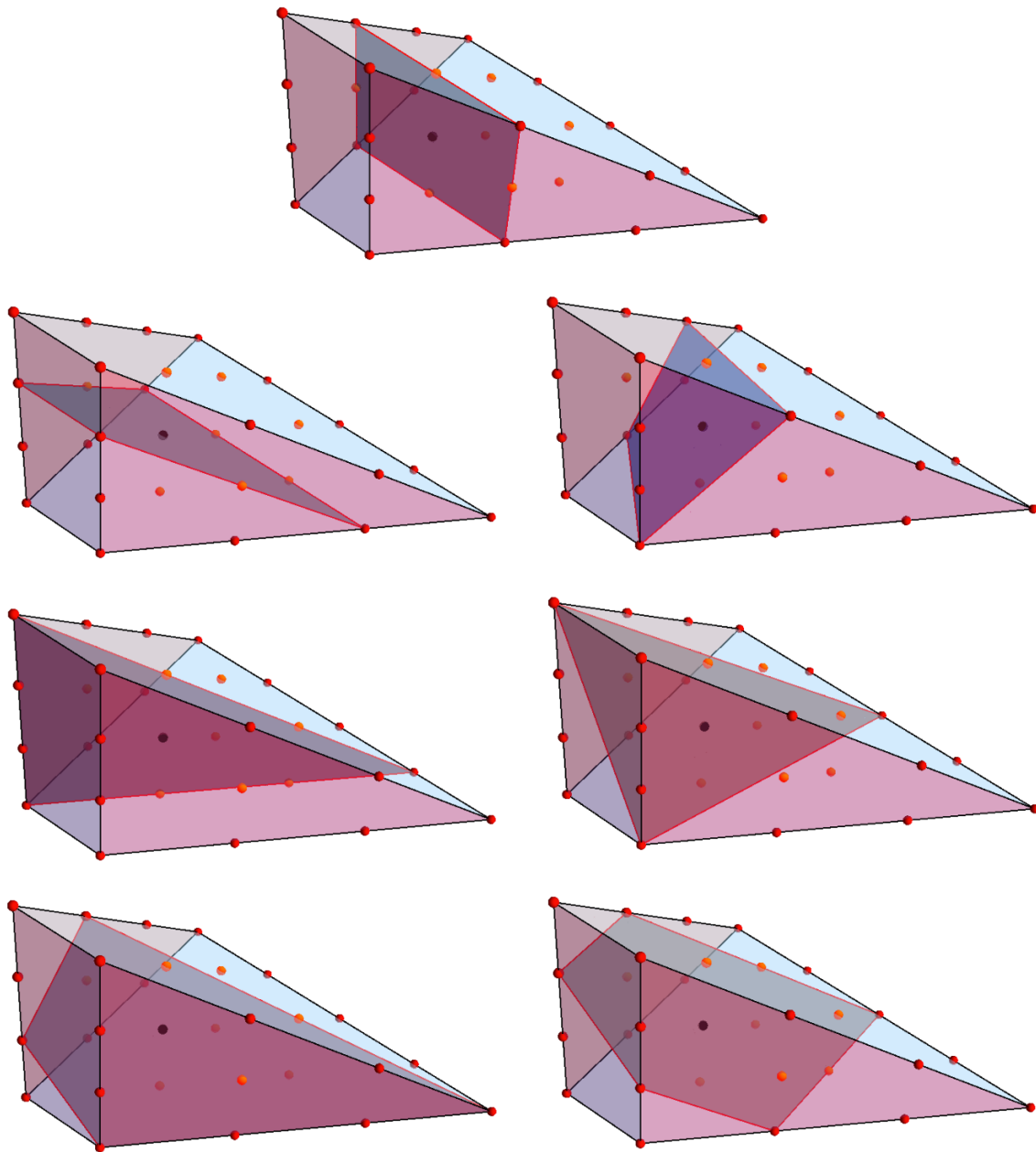


**Figure 17.** The polyhedron  $\nabla$  for the fifth  $K3$  surface. This  $K3$  admits five different elliptic fibration structures, of types  $SO(16) \times SU(8)$ ,  $SO(10) \times SU(11)$ ,  $E_8 \times E_7$ ,  $E_6 \times SU(9)$ ,  $E_8 \times E_8$ ,  $E_6 \times E_7$  and  $SO(14) \times SO(14)$  from top to bottom right.

**The ninth  $K3$ .** The ninth  $K3$  surface is given by a polyhedron  $\nabla$  with vertices

$$w_i = \{(-1, -1, -1), (-1, -1, 1), (1, -1, -1), (-1, 3, 5), (-1, 3, -1)\} \quad (D.23)$$

and its dual  $\Delta$ , with vertices

$$v_a = \{(-2, -1, 0), (-1, 1, -1), (0, 1, 0), (1, 0, 0), (0, 0, 1)\}. \quad (D.24)$$

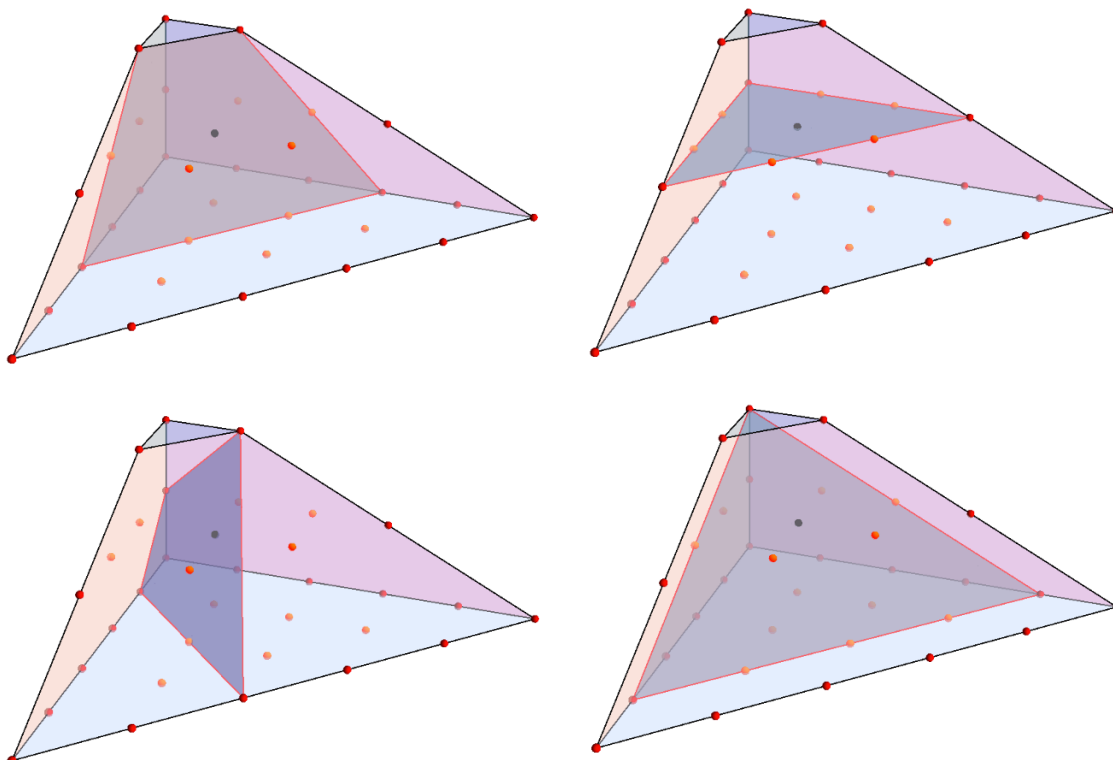


**Figure 18.** The polyhedron  $\nabla$  for the third  $K3$  surface. This  $K3$  admits four different elliptic fibration structures, of types  $SO(18) \times E_6$ ,  $SU(15) \times SU(3)$ ,  $E_8 \times E_7$  and  $E_7 \times SU(10)$ , from top left to bottom right.

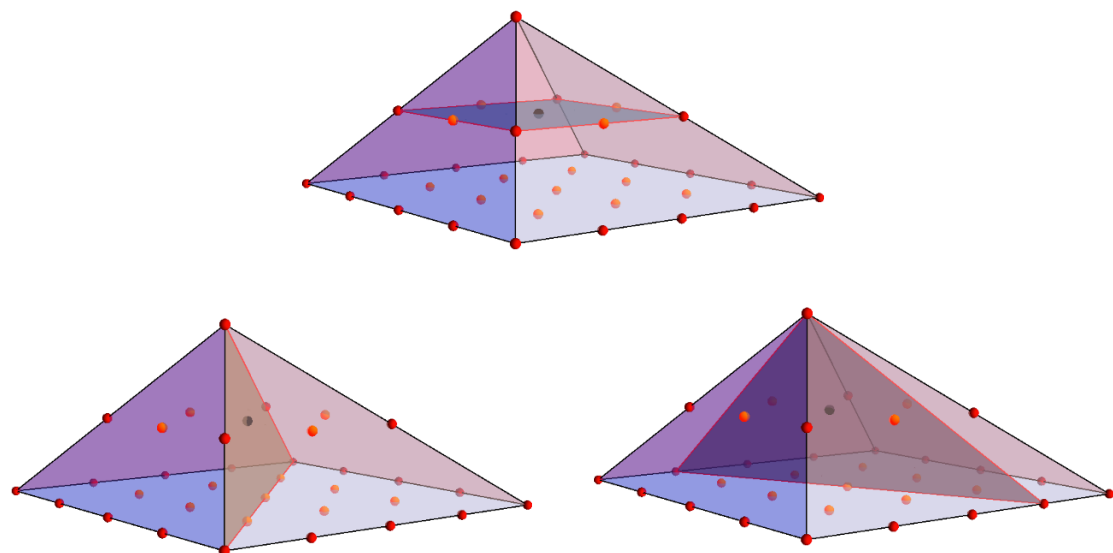


**Figure 19.** The polyhedron  $\nabla$  for the third  $K3$  surface. This  $K3$  admits four different elliptic fibration structures, of types  $\{1\} \times SU(16)$ ,  $E_7 \times E_7$  and  $E_8 \times E_8$ , from top to bottom right.

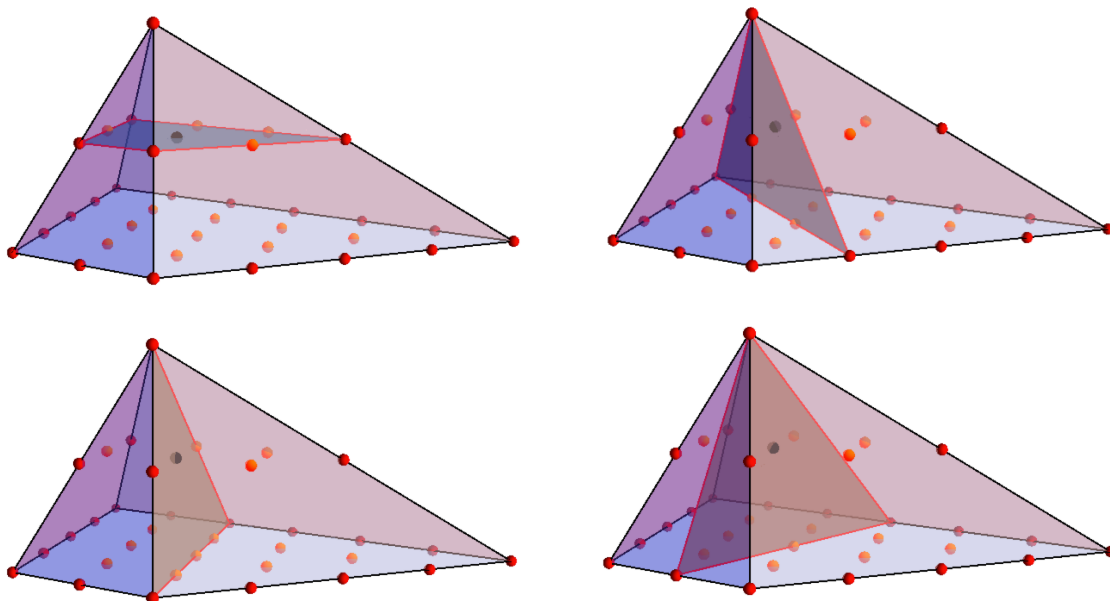


**Figure 20.** The polyhedron  $\nabla$  for the third  $K3$  surface. This  $K3$  admits four different elliptic fibration structures, of types  $\{1\} \times \text{SU}(16)$ ,  $E_8 \times E_7$ ,  $E_7 \times \text{SO}(16)$  and  $E_8 \times E_8$ , from top left to bottom right.

The pair  $(\nabla, \Delta)$  leads, in this case, to the following defining polynomial:

$$f = -c_0 z_1 z_2 z_3 z_4 z_5 + c_1 z_1^4 z_2^4 + c_2 z_4^4 z_5^4 + c_3 z_1^2 z_5^6 + c_4 z_2^2 z_4^6 + c_5 z_3^2 \quad (\text{D.25})$$

**Open Access.** This article is distributed under the terms of the Creative Commons Attribution License ([CC-BY 4.0](https://creativecommons.org/licenses/by/4.0/)), which permits any use, distribution and reproduction in any medium, provided the original author(s) and source are credited.

## References

- [1] P. Candelas, A. Constantin, C. Damian, M. Larfors and J.F. Morales, *Type IIB flux vacua from G-theory II*, [arXiv:1411.4786](https://arxiv.org/abs/1411.4786) [[INSPIRE](#)].
- [2] M. Graña, R. Minasian, M. Petrini and A. Tomasiello, *Supersymmetric backgrounds from generalized Calabi-Yau manifolds*, *JHEP* **08** (2004) 046 [[hep-th/0406137](#)] [[INSPIRE](#)].
- [3] J.M. Maldacena and C. Núñez, *Supergravity description of field theories on curved manifolds and a no go theorem*, *Int. J. Mod. Phys. A* **16** (2001) 822 [[hep-th/0007018](#)] [[INSPIRE](#)].
- [4] S.B. Giddings, S. Kachru and J. Polchinski, *Hierarchies from fluxes in string compactifications*, *Phys. Rev. D* **66** (2002) 106006 [[hep-th/0105097](#)] [[INSPIRE](#)].
- [5] L. Martucci, J.F. Morales and D.R. Pacifici, *Branes, U-folds and hyperelliptic fibrations*, *JHEP* **01** (2013) 145 [[arXiv:1207.6120](#)] [[INSPIRE](#)].
- [6] A.P. Braun, F. Fucito and J.F. Morales, *U-folds as K3 fibrations*, *JHEP* **10** (2013) 154 [[arXiv:1308.0553](#)] [[INSPIRE](#)].



- [7] C. Vafa, *Evidence for F-theory*, *Nucl. Phys. B* **469** (1996) 403 [[hep-th/9602022](#)] [[INSPIRE](#)].
- [8] A. Kumar and C. Vafa, *U manifolds*, *Phys. Lett. B* **396** (1997) 85 [[hep-th/9611007](#)] [[INSPIRE](#)].
- [9] J.T. Liu and R. Minasian, *U-branes and  $T^3$  fibrations*, *Nucl. Phys. B* **510** (1998) 538 [[hep-th/9707125](#)] [[INSPIRE](#)].
- [10] S. Hellerman, J. McGreevy and B. Williams, *Geometric constructions of nongeometric string theories*, *JHEP* **01** (2004) 024 [[hep-th/0208174](#)] [[INSPIRE](#)].
- [11] C.M. Hull, *A geometry for non-geometric string backgrounds*, *JHEP* **10** (2005) 065 [[hep-th/0406102](#)] [[INSPIRE](#)].
- [12] A. Flournoy, B. Wecht and B. Williams, *Constructing nongeometric vacua in string theory*, *Nucl. Phys. B* **706** (2005) 127 [[hep-th/0404217](#)] [[INSPIRE](#)].
- [13] A. Dabholkar and C. Hull, *Generalised T-duality and non-geometric backgrounds*, *JHEP* **05** (2006) 009 [[hep-th/0512005](#)] [[INSPIRE](#)].
- [14] J. Gray and E.J. Hackett-Jones, *On T-folds, G-structures and supersymmetry*, *JHEP* **05** (2006) 071 [[hep-th/0506092](#)] [[INSPIRE](#)].
- [15] C.M. Hull, *Generalised geometry for M-theory*, *JHEP* **07** (2007) 079 [[hep-th/0701203](#)] [[INSPIRE](#)].
- [16] D. Vegh and J. McGreevy, *Semi-flatland*, *JHEP* **10** (2008) 068 [[arXiv:0808.1569](#)] [[INSPIRE](#)].
- [17] P.P. Pacheco and D. Waldram, *M-theory, exceptional generalised geometry and superpotentials*, *JHEP* **09** (2008) 123 [[arXiv:0804.1362](#)] [[INSPIRE](#)].
- [18] M. Graña, R. Minasian, M. Petrini and D. Waldram, *T-duality, generalized geometry and non-geometric backgrounds*, *JHEP* **04** (2009) 075 [[arXiv:0807.4527](#)] [[INSPIRE](#)].
- [19] J. McOrist, D.R. Morrison and S. Sethi, *Geometries, non-geometries and fluxes*, *Adv. Theor. Math. Phys.* **14** (2010) [[arXiv:1004.5447](#)] [[INSPIRE](#)].
- [20] D. Andriot, M. Larfors, D. Lüst and P. Patalong, *A ten-dimensional action for non-geometric fluxes*, *JHEP* **09** (2011) 134 [[arXiv:1106.4015](#)] [[INSPIRE](#)].
- [21] A. Coimbra, C. Strickland-Constable and D. Waldram, *Supergravity as generalised geometry I: type II theories*, *JHEP* **11** (2011) 091 [[arXiv:1107.1733](#)] [[INSPIRE](#)].
- [22] D.S. Berman, H. Godazgar, M. Godazgar and M.J. Perry, *The local symmetries of M-theory and their formulation in generalised geometry*, *JHEP* **01** (2012) 012 [[arXiv:1110.3930](#)] [[INSPIRE](#)].
- [23] D.S. Berman, H. Godazgar, M.J. Perry and P. West, *Duality invariant actions and generalised geometry*, *JHEP* **02** (2012) 108 [[arXiv:1111.0459](#)] [[INSPIRE](#)].
- [24] A. Coimbra, C. Strickland-Constable and D. Waldram,  *$E_{d(d)} \times \mathbb{R}^+$  generalised geometry, connections and M-theory*, *JHEP* **02** (2014) 054 [[arXiv:1112.3989](#)] [[INSPIRE](#)].
- [25] O. Hohm and B. Zwiebach, *On the Riemann tensor in double field theory*, *JHEP* **05** (2012) 126 [[arXiv:1112.5296](#)] [[INSPIRE](#)].
- [26] D. Andriot, O. Hohm, M. Larfors, D. Lüst and P. Patalong, *A geometric action for non-geometric fluxes*, *Phys. Rev. Lett.* **108** (2012) 261602 [[arXiv:1202.3060](#)] [[INSPIRE](#)].

- [27] D. Andriot, O. Hohm, M. Larfors, D. Lüüst and P. Patalong, *Non-geometric fluxes in supergravity and double field theory*, *Fortsch. Phys.* **60** (2012) 1150 [[arXiv:1204.1979](#)] [[INSPIRE](#)].
- [28] R. Blumenhagen, A. Deser, E. Plauschinn and F. Rennecke, *Non-geometric strings, symplectic gravity and differential geometry of Lie algebroids*, *JHEP* **02** (2013) 122 [[arXiv:1211.0030](#)] [[INSPIRE](#)].
- [29] A. Coimbra, C. Strickland-Constable and D. Waldram, *Supergravity as generalised geometry II:  $E_{d(d)} \times \mathbb{R}^+$  and M-theory*, *JHEP* **03** (2014) 019 [[arXiv:1212.1586](#)] [[INSPIRE](#)].
- [30] G. Aldazabal, M. Graña, D. Marqués and J.A. Rosabal, *Extended geometry and gauged maximal supergravity*, *JHEP* **06** (2013) 046 [[arXiv:1302.5419](#)] [[INSPIRE](#)].
- [31] M. Cederwall, J. Edlund and A. Karlsson, *Exceptional geometry and tensor fields*, *JHEP* **07** (2013) 028 [[arXiv:1302.6736](#)] [[INSPIRE](#)].
- [32] R. Blumenhagen, A. Deser, E. Plauschinn, F. Rennecke and C. Schmid, *The intriguing structure of non-geometric frames in string theory*, *Fortsch. Phys.* **61** (2013) 893 [[arXiv:1304.2784](#)] [[INSPIRE](#)].
- [33] D. Andriot and A. Betz,  *$\beta$ -supergravity: a ten-dimensional theory with non-geometric fluxes and its geometric framework*, *JHEP* **12** (2013) 083 [[arXiv:1306.4381](#)] [[INSPIRE](#)].
- [34] M. Cederwall, *T-duality and non-geometric solutions from double geometry*, *Fortsch. Phys.* **62** (2014) 942 [[arXiv:1409.4463](#)] [[INSPIRE](#)].
- [35] J. de Boer and M. Shigemori, *Exotic branes in string theory*, *Phys. Rept.* **532** (2013) 65 [[arXiv:1209.6056](#)] [[INSPIRE](#)].
- [36] N.J. Hitchin, *The geometry of three-forms in six and seven dimensions*, [math/0010054](#) [[INSPIRE](#)].
- [37] M. Larfors, D. Lüüst and D. Tsimpis, *Flux compactification on smooth, compact three-dimensional toric varieties*, *JHEP* **07** (2010) 073 [[arXiv:1005.2194](#)] [[INSPIRE](#)].
- [38] T.H. Buscher, *A symmetry of the string background field equations*, *Phys. Lett. B* **194** (1987) 59 [[INSPIRE](#)].
- [39] T.H. Buscher, *Path integral derivation of quantum duality in nonlinear  $\sigma$ -models*, *Phys. Lett. B* **201** (1988) 466 [[INSPIRE](#)].
- [40] O. Lunin and S.D. Mathur, *Metric of the multiply wound rotating string*, *Nucl. Phys. B* **610** (2001) 49 [[hep-th/0105136](#)] [[INSPIRE](#)].
- [41] P.S. Aspinwall, *K3 surfaces and string duality*, [hep-th/9611137](#) [[INSPIRE](#)].
- [42] B.R. Greene, A.D. Shapere, C. Vafa and S.-T. Yau, *Stringy cosmic strings and noncompact Calabi-Yau manifolds*, *Nucl. Phys. B* **337** (1990) 1 [[INSPIRE](#)].
- [43] V.V. Batyrev, *Dual polyhedra and mirror symmetry for Calabi-Yau hypersurfaces in toric varieties*, *J. Alg. Geom.* **3** (1994) 493 [[alg-geom/9310003](#)] [[INSPIRE](#)].
- [44] M. Kreuzer and H. Skarke, *Classification of reflexive polyhedra in three-dimensions*, *Adv. Theor. Math. Phys.* **2** (1998) 847 [[hep-th/9805190](#)] [[INSPIRE](#)].
- [45] P. Berglund et al., *Periods for Calabi-Yau and Landau-Ginzburg vacua*, *Nucl. Phys. B* **419** (1994) 352 [[hep-th/9308005](#)] [[INSPIRE](#)].
- [46] P. Griffiths, *On the periods of certain rational integrals. I*, *Ann. Math.* **90** (1969) 460.

- [47] P. Griffiths, *On the periods of certain rational integrals. II*, *Ann. Math.* **90** (1969) 466.
- [48] D.R. Morrison, *Picard-Fuchs equations and mirror maps for hypersurfaces*, [hep-th/9111025](#) [[INSPIRE](#)].
- [49] P. Candelas, X. De La Ossa, A. Font, S.H. Katz and D.R. Morrison, *Mirror symmetry for two parameter models. 1.*, *Nucl. Phys. B* **416** (1994) 481 [[hep-th/9308083](#)] [[INSPIRE](#)].
- [50] P. Candelas, A. Font, S.H. Katz and D.R. Morrison, *Mirror symmetry for two parameter models. 2.*, *Nucl. Phys. B* **429** (1994) 626 [[hep-th/9403187](#)] [[INSPIRE](#)].
- [51] S. Hosono, A. Klemm, S. Theisen and S.-T. Yau, *Mirror symmetry, mirror map and applications to complete intersection Calabi-Yau spaces*, *Nucl. Phys. B* **433** (1995) 501 [[hep-th/9406055](#)] [[INSPIRE](#)].
- [52] S. Hosono, A. Klemm, S. Theisen and S.-T. Yau, *Mirror symmetry, mirror map and applications to Calabi-Yau hypersurfaces*, *Commun. Math. Phys.* **167** (1995) 301 [[hep-th/9308122](#)] [[INSPIRE](#)].
- [53] M. Bianchi, J.F. Morales and G. Pradisi, *Discrete torsion in nongeometric orbifolds and their open string descendants*, *Nucl. Phys. B* **573** (2000) 314 [[hep-th/9910228](#)] [[INSPIRE](#)].
- [54] V. Braun, *Toric elliptic fibrations and F-theory compactifications*, *JHEP* **01** (2013) 016 [[arXiv:1110.4883](#)] [[INSPIRE](#)].
- [55] A. Malmendier and D.R. Morrison, *K3 surfaces, modular forms and non-geometric heterotic compactifications*, [arXiv:1406.4873](#) [[INSPIRE](#)].
- [56] M. Billó et al., *Non-perturbative gauge/gravity correspondence in  $N = 2$  theories*, *JHEP* **08** (2012) 166 [[arXiv:1206.3914](#)] [[INSPIRE](#)].
- [57] W. Fulton, *Introduction to toric varieties. The 1989 William H. Roever lectures in geometry*, Annals of Mathematics Studies volume 131, Princeton University Press, Princeton U.S.A. (1993).
- [58] D.A. Cox, J.B. Little and H.K. Schenck, *Toric varieties*, Graduate Studies In Mathematics volume 124, American Mathematical Society, U.S.A. (2011).
- [59] H. Skarke, *String dualities and toric geometry: an introduction*, *Chaos Solitons Fractals* **10** (1999) 543 [[hep-th/9806059](#)] [[INSPIRE](#)].
- [60] A.C. Avram, M. Kreuzer, M. Mandelberg and H. Skarke, *Searching for K3 fibrations*, *Nucl. Phys. B* **494** (1997) 567 [[hep-th/9610154](#)] [[INSPIRE](#)].
- [61] P. Candelas and A. Font, *Duality between the webs of heterotic and type-II vacua*, *Nucl. Phys. B* **511** (1998) 295 [[hep-th/9603170](#)] [[INSPIRE](#)].
- [62] P. Candelas and H. Skarke, *F theory, SO(32) and toric geometry*, *Phys. Lett. B* **413** (1997) 63 [[hep-th/9706226](#)] [[INSPIRE](#)].
- [63] P. Candelas, A. Constantin and H. Skarke, *An abundance of K3 fibrations from polyhedra with interchangeable parts*, *Commun. Math. Phys.* **324** (2013) 937 [[arXiv:1207.4792](#)] [[INSPIRE](#)].
- [64] M. Kreuzer and H. Skarke, *Calabi-Yau four folds and toric fibrations*, *J. Geom. Phys.* **26** (1998) 272 [[hep-th/9701175](#)] [[INSPIRE](#)].
- [65] D. Chialva, U.H. Danielsson, N. Johansson, M. Larfors and M. Vonk, *Deforming, revolving and resolving — New paths in the string theory landscape*, *JHEP* **02** (2008) 016 [[arXiv:0710.0620](#)] [[INSPIRE](#)].